Chapter 7. Terrestrial Carbon Modeling: Baseline and Projections in Lowland Ecosystems of Alaska

By Yujie He,[1] Hélène Genet,[2] A. David McGuire,[3] Qianlai Zhuang,[1] Bruce K. Wylie,[4] and Yujin Zhang[2]

7.1. Highlights

- The total area of wetland in Alaska was estimated at 177,069 square kilometers (km^2), which represents nearly 12 percent of the total land surface area (including uplands and inland waters) of the State.
- During the historical period (1950–2009), wetland ecosystems in Alaska lost carbon at a rate of 1.3 teragrams of carbon per year (TgC/yr). The loss was the result of the net carbon source in the Northwest Boreal Landscape Conservation Cooperative (LCC) North, which overrode gains in all other LCC regions in Alaska to yield a net carbon loss statewide.
- Historical biogenic and pyrogenic methane (CH_4) emissions from Alaska wetland ecosystems were estimated to average about 27.93 teragrams of carbon dioxide equivalent per year ($TgCO_2$-eq/yr) and 0.466 $TgCO_2$-eq/yr during the 1950s, respectively. Biogenic and pyrogenic CH_4 emissions significantly increased from 1950 through 2009 by 0.977 grams of carbon dioxide equivalent per square meter per year (gCO_2-eq/m^2/yr) and 0.037 gCO_2-eq/m^2/yr, respectively. The global warming potential (GWP) of wetlands over the historical period indicates a significant source of greenhouse gas forcing of 33 $TgCO_2$-eq/yr.
- By the end of the 21st century, wetland ecosystems of all LCC regions of Alaska were projected to gain carbon, storing between 3.0 and 5.3 TgC/yr statewide by the 2090s, depending on the climate change simulations used in the assessment.
- Future mean annual CH_4 emissions are estimated to range from 37 to 90 $TgCO_2$-eq/yr by 2090–2099, depending on the climate change simulations used in the assessment, representing an increase of 15 to 182 percent compared with those of 2000–2009. The large warming potential of CH_4 emissions would be enough to offset the cooling effect of carbon gain statewide. The average annual GWP of wetlands over the projection period indicates a potential significant source of greenhouse gas forcing of 17 to 64 $TgCO_2$-eq/yr, despite the net carbon storage to wetland ecosystems.
- Biogenic CH_4 emissions during the historical and future periods were found to be positively correlated with the atmospheric carbon dioxide (CO_2) concentrations; future CH_4 emissions were also projected to be significantly influenced by mean annual temperature.

7.2. Introduction

Wetlands accumulate peat owing to positive net ecosystem carbon balance, where net primary productivity and associated litterfall exceeds soil carbon loss from decomposition and methane production (Frolking and Roulet, 2007). Methane (CH_4) is currently the second most important anthropogenic greenhouse gas, for which wetlands are the single largest natural source. CH_4 emissions from high-latitude wetlands are an important component of the global climate system (Fisher and others, 2014). There is major concern about potential feedbacks between the climate system and CH_4 emissions from wetlands, as climate, atmospheric carbon dioxide (CO_2) concentrations, and deposition of sulfate and nitrogen are all known to affect CH_4 emissions positively or negatively (Forster and others, 2007). There is compelling evidence that CH_4 emissions from wetlands have been strongly responsive to climate

[1]Purdue University, West Lafayette, Ind.

[2]University of Alaska-Fairbanks, Fairbanks, Alaska.

[3]U.S. Geological Survey, Fairbanks, Alaska.

[4]U.S. Geological Survey, Sioux Falls, S. Dak.

in the past (He and others, 2014) and will likely continue to be responsive to anthropogenically driven climate change in the future. The high sensitivity of CH_4 emissions to soil temperature and moisture conditions and its subsequent effect on the climate system is an important issue to assess in northern high latitudes, because this region contains nearly half of the world's wetlands (Lehner and Döll, 2004) and because high latitudes have been and are forecast to continue experiencing more rapid warming than elsewhere (Stocker and others, 2013). Another concern is the potential release of previously frozen, labile soil carbon from thawing permafrost in the form of CO_2 and (or) CH_4 through mineralization owing to climate warming over the next century (Schuur and others, 2008; Koven and others, 2011; Schaefer and others, 2011).

In addition to high vulnerability for carbon loss from CH_4 production, wetlands, especially in boreal regions, are susceptible to carbon loss from wildfires. Wetlands generally burn less frequently than uplands because poorly drained conditions are responsible for low flammability, which minimizes fire activity in wetlands compared with better drained uplands. However, extended periods of dry weather along with increased occurrence of late-season burning (Kasischke and Turetsky, 2006) and changes in drainage conditions have the potential to trigger deep organic soil burning in wetlands (Turetsky and others, 2011), making these ecosystems potentially more vulnerable to fire and carbon loss. Wetland distribution also has local effects on wildlife habitat and subsistence resources (Grand and others, 1997). For instance, wetlands are refuges to a number of waterbird species that migrate from across the world to breed in the wetlands of Alaska (Martin and others, 2009). Wetlands are also an important habitat for moose, which represent an important source of food for local populations (Martin and others, 2009). Because of their importance in local and regional carbon dynamics and biodiversity, accurate distribution of wetlands across Alaska is of great importance. However, mapping wetlands in Alaska using remote sensing is challenging, and specific wetland classes, such as bogs, are particularly difficult to discriminate because woody overstory vegetation can block understory wetland vegetation and surface water. To assess carbon dynamics in the wetlands of Alaska, we developed a wetland distribution map that separated bogs and fens using the Alaska National Wetlands Inventory as a reference dataset.

In this chapter, we present a modeling synthesis of changes in carbon stocks and CH_4 emissions and other carbon fluxes among the soil, the vegetation, and the atmosphere over the historical period (1950–2009) and projection period (2010–2099) for Alaska. The modeling framework we used in this assessment couples a wildfire disturbance model with two process-based ecosystem models to estimate current and projected carbon stocks and CO_2 and CH_4 fluxes for wetlands in Alaska. Projections were made for two climate models that simulated future climates for each of three different CO_2 emissions scenarios to estimate uncertainties in future climate forcing. We used the wetland distribution map to quantify CH_4 emissions over the historical and future time period in Alaska.

7.3. Methods

7.3.1. Methane Dynamics Module of the Terrestrial Ecosystem Model (MDM-TEM) Description

Changes in soil and vegetation carbon stocks and CO_2 fluxes in response to climate change and disturbances were simulated using a modeling framework that couples the output of a wildfire disturbance model, the Alaska Frame-Based Ecosystem Code (ALFRESCO; Rupp and others, 2000, 2002, 2007; see chapter 2), to a process-based ecosystem model that simulates carbon and nitrogen pools and CO_2 dynamics, the Dynamic Organic Soil version of the Terrestrial Ecosystem Model (DOS-TEM; Yi, Manies, and others, 2009; Yi, McGuire, and others, 2009; Yi and others, 2010; Genet and others, 2013; see chapter 6). Changes in biogenic CH_4 fluxes were simulated by coupling the output of DOS-TEM with the Methane Dynamics Module (MDM) of the Terrestrial Ecosystem Model (MDM-TEM; Zhuang and others, 2004). The ALFRESCO and DOS-TEM aspects of the model framework used in this assessment are described in chapters 2 and 6. Here we will provide a detailed description of MDM-TEM. MDM-TEM simulates biogenic CH_4 dynamics at daily timesteps for the Terrestrial Ecosystem Model (TEM) and explicitly considers the process of CH_4 production (methanogenesis) as well as CH_4 oxidation (methanotrophy) and the transport of the gas from the soil to the atmosphere (Zhuang and others, 2004). The MDM has been coupled to several existing TEM modules, including the core carbon and nitrogen dynamics module (Zhuang and others, 2003), the soil thermal module that incorporates permafrost dynamics (Zhuang and others, 2001), and a hydrological module that simulates water movements across an atmosphere-vegetation-soil continuum (Zhuang and others, 2002, 2004). Specifically, the soil component of the hydrological module considers moisture dynamics explicitly in moss, organic soil, and mineral soil layers (Zhuang and others, 2002, 2004), and is designed to consider fluctuations in water table depth.

In the MDM-TEM, the fluxes of CH_4 between soils and the atmosphere depend on the relative rates of CH_4 production and oxidation within the soil profile and the transport of CH_4 across the surface of soils. The soil in the model is separated into an upper unsaturated zone and a lower saturated zone according to the water table depth. The net emissions (or uptake) of CH_4 between the soil and the atmosphere are the balance between CH_4 production and oxidation. If the rate of production is larger than the rate of oxidation within the soil profile, CH_4 will be emitted to the atmosphere through diffusion. In wetland ecosystems, two other pathways in addition to diffusion are important for CH_4 transport to the atmosphere. One is plant-aided transport, where CH_4 can move through aerenchyma tissues (that is, "hollow tubes") that run from the roots through the stems to the leaves of some plants. Another is ebullition, where a high concentration of CH_4 causes the formation of CH_4 bubbles that can move through the overlying water or soils and escape into the atmosphere.

CH_4 production is modeled as an anaerobic process that occurs in the saturated zone of the soil profile and is influenced by (1) substrate availability, which is a function of net primary productivity of the overlying vegetation from DOS-TEM wetland/lowland simulations (see more detail below); (2) soil temperature, which uses a Q_{10} function (Q_{10} denotes the change in biogeochemical process rate per 10 °C change in temperature) with a reference temperature and Q_{10} coefficients that vary across ecosystems; (3) soil pH, where the optimum is set to 7.5; and (4) the availability of electron acceptors related to the effects of redox potential. CH_4 oxidation is modeled as an aerobic process that occurs in the unsaturated zone of the soil profile and is influenced by (1) soil temperature and redox potential, (2) substrate availability via a Michaelis-Menten function, and (3) soil moisture, which diminishes oxidation above the optimum soil moisture for oxidation.

7.3.2. Model Parameterization and Validation

7.3.2.1. Wetland Classification

Wetlands are ecosystems that are waterlogged seasonally or year-round. Wetland ecosystems are characterized by poor drainage conditions and a thick organic layer (see table 7.1). Wetlands in tundra regions of the Arctic and Western Alaska Landscape Conservation Cooperatives (LCCs) are composed primarily of graminoid tundra and wet-sedge tundra. In the Arctic LCC, tundra wetland regions consisted of 84.7 percent graminoid tundra and 15.3 percent wet-sedge tundra. In the Western Alaska LCC, tundra wetland regions consisted of 27.6 percent graminoid tundra and 72.4 percent wet-sedge tundra. In the Northwest Boreal LCC, wetlands consisted of 97 percent lowland permafrost plateau forest (46 percent evergreen forest and 51 percent deciduous forest) and 3 percent treeless ecosystems (that is, bogs and fens). Bogs and fens are especially important to assessing CH_4 dynamics owing to their high emissions. Because treeless wetlands were not extensive in the region, we used the parameterization for graminoid tundra for the simulation of these land-cover types. In the North Pacific LCC, wetlands consisted of 86 percent maritime fen and 14 percent maritime wetland forest (dominated by Sitka spruce [*Picea sitchensis* (Bong.) Carrière] and black cottonwood [*Populus trichocarpa* Torr. & A. Gray ex Hook.]).

7.3.2.2. Methane Dynamics Module of the Terrestrial Ecosystem Model (MDM-TEM)

MDM-TEM is parameterized for three different types of wetland (table 7.2) based on specific vegetation and hydrological characteristics. Therefore, the seven wetland land-cover types for the vegetation map were identified with three MDM-TEM parameterizations. Specifically, (1) lowland black spruce (*Picea mariana* (Mill.) Britton, Sterns & Poggenb.), white spruce (*Picea glauca* (Moench) Voss), and deciduous forests and maritime wetland forest were identified with the boreal forest wetland category from MDM-TEM; (2) graminoid tundra was identified with the alpine tundra wetland category from MDM-TEM; and (3) wet-sedge tundra and maritime fen were identified with the moist tundra wetland category from MDM-TEM. The MDM-TEM was parameterized using CH_4 measurements and soil and climate factors from three wetland field sites in arctic tundra and Canadian wetland (first three sites in table 7.2). The MDM-TEM was parameterized by minimizing the differences between observed fluxes and simulated fluxes at the Toolik-D, Toolik-W (Arctic LCC, Alaska), and SSA-FEN (Saskatchewan, Canada) field sites. For each site, the model was initialized by a set of parameter values determined by a literature review. Each individual parameter was bounded by the ranges of values from the literature review and then

Table 7.1. Target values for carbon pool and flux variables used to calibrate the Dynamic Organic Soil version of the Terrestrial Ecosystem Model (DOS-TEM) for major wetland land-cover types in Alaska.

[Soil mineral carbon pools are estimated from the bottom of the organic layer down to 1 meter into the mineral soil. $gC/m^2/yr$, gram of carbon per square meter per year; gC/m^2, gram of carbon per square meter; —, not applicable]

Wetland land-cover type	Net primary productivity ($gC/m^2/yr$)	Carbon pool (gC/m^2)			
		Vegetation	Soil fibric	Soil humic	Soil mineral
Boreal lowland black spruce forest	103	2,105	2,432	10,757	19,821
Boreal lowland white spruce forest	259	4,180	1,875	8,311	11,005
Boreal lowland deciduous forest	299	6,673	1,243	5,523	11,005
Graminoid	112	561	3,079	7,703	43,403
Wet-sedge tundra	54	458	3,358	8,401	44,252
Maritime forested wetland	893	16,344	1,666	28,666	10,380
Maritime fen	113	960	2,666	59,115	—

Table 7.2. Description of sites used in the model parameterization and validation process.

[MDM-TEM, Methane Dynamics Module of the Terrestrial Ecosystem Model; BOREAS, Boreal Ecosystem-Atmosphere Study]

Site name	Location	Elevation (meters)	Land cover	Wetland type in MDM-TEM	Observed data
Tundra at Toolik Field Station (Toolik-D)	149°36' W. 68°38' N.	760	Tussock tundra	Alpine tundra wetland	Soil temperatures at depths of 10, 20, and 50 centimeters, methane fluxes from 1992 and 1993
Tundra at Toolik Field Station (Toolik-W)	149°36' W. 68°38' N.	760	Wet tussock tundra	Moist tundra wetland	Soil temperatures at depths of 3, 5, 7, 9, and 11 centimeters, methane fluxes from 1994 and 1995
Fen at southern study area of BOREAS (SSA-FEN)	105°57' W. 53°57' N.	524.7	Complex fen with buckbean, sedges, birch, and willow	Boreal forest wetland	Soil temperatures at depths of 10 and 20 centimeters, daily evapotranspiration and eddy covariance measurements of methane fluxes for May to October of 1994 and 1995
Fen at northern study area of BOREAS (NSA-FEN; validation site)	98°25' W. 55°55' N.	218	Fen complex including sedge, moss, moat, and shrubs	Boreal forest wetland	Soil temperatures at depths of 5, 10, 20, 50, and 100 centimeters; water-table depth (1994) and chamber measurements of methane fluxes of May through September 1994 and June through October 1996

adjusted so that the root mean square error (RMSE) between the daily simulated and observed CH_4 fluxes was minimized. This procedure was conducted sequentially for all parameters until the minimized RMSE for the Toolik-D, Toolik-W, and SSA-FEN sites were 665 milligrams of carbon dioxide equivalent per square meter per day ($mgCO_2$-eq/m^2/d), 1,729 $mgCO_2$-eq/m^2/d, and 1,396 $mgCO_2$-eq/m^2/d, respectively.

7.3.2.3. Dynamic Organic Soil Version of the Terrestrial Ecosystem Model (DOS-TEM)

Wetland land-cover types considered in DOS-TEM include wet-sedge and graminoid tundra; black spruce, white spruce, and deciduous lowland boreal forests; and maritime wetland forest and maritime fen. We calibrated the rate-limiting parameters of DOS-TEM using target values of carbon and nitrogen pools and fluxes representative of mature ecosystems. These parameters are "tuned" until the model reaches target values of the main carbon and nitrogen pools and fluxes (Clein and others, 2002). The calibration of these parameters is an effective way of dealing with temporal scaling issues in ecosystem models (Rastetter and others, 1992). For boreal forest communities, an existing set of target values for vegetation and soil carbon and nitrogen pools and fluxes were assembled using data collected in the Bonanza Creek Long Term Ecological Research (LTER) program (Yuan and others, 2012). For tundra communities, we used data collected at the Toolik Field Station (Shaver and Chapin, 1991; Van Wijk and others, 2003; Sullivan and others, 2007; Euskirchen and others, 2012; Gough and others, 2012; Sistla and others, 2013). For the maritime and boreal-lowland-forest communities, we used data summarized in chapter 4, collected within three watersheds located near Juneau, Alaska, with mean annual precipitation of 1,580 millimeters (mm) and mean monthly average temperatures ranging from 2 to 9 degrees Celsius (°C) (see chapter 4, section 4.3.1 for details). Target values of vegetation biomass, soil carbon pools, and net primary productivity for each wetland land-cover type are described in table 7.1.

7.3.2.4. Model Validation

Model validation consists of testing the ability of a model to extrapolate carbon dynamics across space and time. It consists of comparing model simulations with observations collected at sites and times independent of the data used for model parameterization and calibration. When independent observations are not available, model verification consists of testing the ability of the model to reproduce the data used for calibration.

For MDM-TEM, the wetland parameterization was validated at the NSA-FEN site in Canada using the parameterization from SSA-FEN site (table 7.2). A geometric mean regression between the simulated monthly mean and observed net emissions was significant ($p < 0.01$; $n = 10$ months; where p denotes p-value, n denotes number of observations) with coefficient of determination, $R^2 = 0.90$; slope $= 24.3 \pm 2.3$ grams of carbon dioxide equivalent per square meter per month (gCO_2-eq/m^2/mo); and intercept $= 11.6 \pm 7.7$ gCO_2-eq/m^2/mo.

DOS-TEM parameterization has been validated using soil and vegetation biomass data derived from field observations

independent of the data used for model parameterization. The National Soil Carbon Network database for Alaska was used to validate DOS-TEM estimates of soil carbon stocks (Johnson and others, 2011). In order to compare similar estimates from model and observation, only deep profiles were selected from the database—that is, profiles with a description of the entire organic layer and the 90- to 110-centimeter (cm)-thick mineral layer beneath the organic layer.

Estimates of vegetation carbon stocks for tundra wetlands were compared with observations recorded in the data catalog of the Arctic LTER at Toolik Field Station (http://toolik.alaska.edu; Shaver and Chapin, 1986). For the boreal forest wetlands, vegetation carbon stocks simulated by DOS-TEM were compared with estimates from forest inventories conducted by the Cooperative Alaska Forest Inventory (Malone and others, 2009). The forest inventory only provided estimates of aboveground biomass. Aboveground biomass was converted to total biomass by using a ratio of aboveground versus total biomass of 0.8 in forest and 0.6 in tundra ecosystems. Carbon content of the biomass was estimated at 50 percent.

Finally, for maritime fen and maritime wetland forests, model validation was not possible as no additional independent data were available in this region. For these wetland ecosystems, we compared the model simulations with observed data at the same sites that were used for model parameterization. (See chapter 4, section 4.3.1 for site descriptions).

7.4. Model Application and Analysis

Spatially explicit data for climate, land cover, and soil texture were used to drive DOS-TEM and MDM-TEM. In addition, MDM-TEM used DOS-TEM estimates of monthly net primary productivity (NPP) and leaf area index (LAI) to simulate CH_4 dynamics. Because MDM-TEM runs at a daily timestep, the monthly forcing data were interpolated to daily timesteps within MDM-TEM (Zhuang and others, 2004). Chapter 6, section 6.3.4.2 provides descriptions of these data sources. To evaluate the effects of historical and projected climate warming, we conducted a series of six climate simulations combining (1) historical climate variability from 1901 through 2009 using Climatic Research Unit (CRU TS v. 3.10.01; Harris and others, 2014; www.cru.uea.ac.uk/) data and (2) climate variability from 2010 through 2099 projected by two general circulation models (GCMs): version 3.1-T47 of the Coupled Global Climate Model (CGCM3.1, www.cccma.ec.gc.ca/data/cgcm3/; McFarlane and others, 1992; Flato, 2005) developed by the Canadian Centre for Climate Modelling and Analysis and version 5 of the European Centre Hamburg Model (ECHAM5, www.mpimet.mpg.de/en/wissenschaft/modelle/echam/; Roeckner and others, 2003, 2004) developed by the Max Planck Institute. The climate projections were aligned with the Intergovernmental Panel on Climate Change's Special Report on Emissions Scenarios (IPCC-SRES; Nakićenović and Swart, 2000). The assessment used three low-, mid- and high-range CO_2 emissions scenarios (B1, A1B, and A2; see further details in chapter 2, section 2.2.1.). A new wetland distribution map of Alaska was developed for this study (see section 7.4.1 below) based on the National Wetlands Inventory (fig. 7.1) and used for both DOS-TEM and MDM-TEM to represent wetland ecosystem distribution (fig. 7.2). The heterogeneity and small clumped nature of wetlands was not possible to reproduce at a 1-kilometer (km) resolution. Therefore, the original wetland map was developed at a 30-meter (m) resolution, and percent cover of wetland was computed for each 1-km pixel.

7.4.1. Development of an Alaska Wetland Distribution Map

In this effort, we developed a new wetland distribution map that separated bogs and fens (fig. 7.2). The Alaska National Wetlands Inventory (NWI; http://www.fws.gov/wetlands/Data/State-Downloads.html) was used as a reference dataset (fig. 7.1), which helped with the development of a representative mapping model to estimate bog and fen distribution. Model development was conducted using a machine-learning, data-driven, nonparametric classification approach driven by Web-enabled Landsat Data spectral and derived indices and ancillary spatially explicit data (table 7.3). Bogs are generally flooded seasonally during spring melt. From the comparison of the NWI classification with field observations collected in the boreal and arctic regions of Alaska, we assumed bogs were identified as saturated scrub shrub in the NWI database because of the presence of dwarf shrubs and mosses. The NWI palustrine codes SS4B (scrub-shrub, needle-leaved, saturated), SS1E (scrub-shrub, broad-leaved, seasonally flooded/saturated), and SS7B (scrub-shrub, deciduous, saturated) were therefore used to define bogs. Fens are generally flooded throughout the growing season. We therefore assumed they were identified as persistent emergent wetlands—that is, the NWI palustrine codes EM1F (emergent, broad-leaved, semipermanently flooded) and EM1E (emergent, broad-leaved, seasonally flooded/saturated).

The wetland distribution map was developed based on a random selection of 18,024 pixels. A database for these pixels was built based on spatial inputs and NWI classes. Attributes from each of the potential input layers (table 7.3) were extracted for each pixel. Out of this set of pixels, 1,030 pixels were randomly selected and withheld for testing purposes. As an additional model sensitivity test, a twentyfold cross-validation was conducted on the model development dataset.

Winnowing was used to select a subset of relevant input spatial variables (Kivinen and others, 1997). A tenfold boosted regression tree (Sutton, 2005), which used the subset of winnowed variables, was developed (table 7.4). Overall accuracies were 75 percent for the independent test and

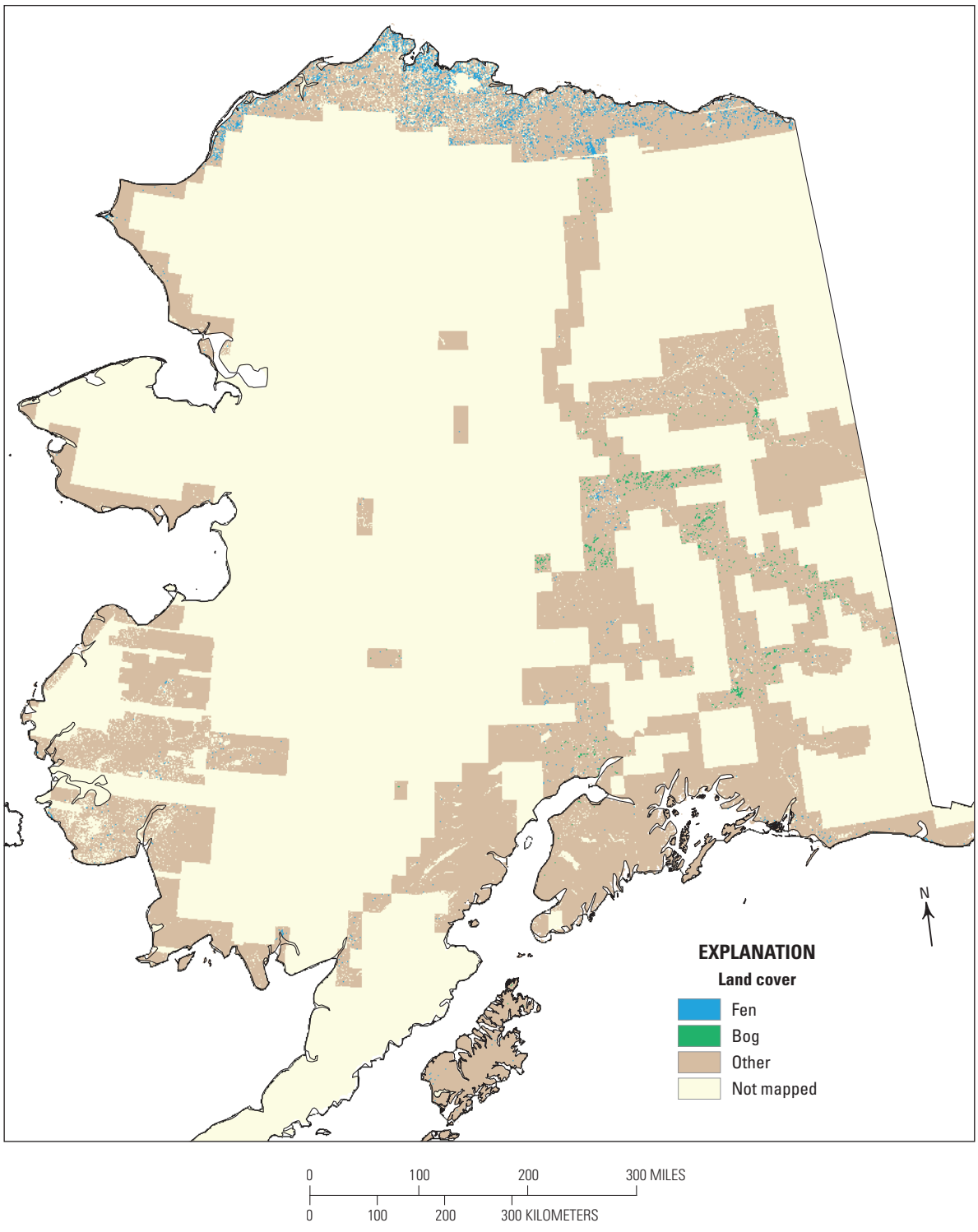

Figure 7.1. National Wetland Inventory data distribution and bog and fen distributions used for the development of an Alaska-wide mapping algorithm.

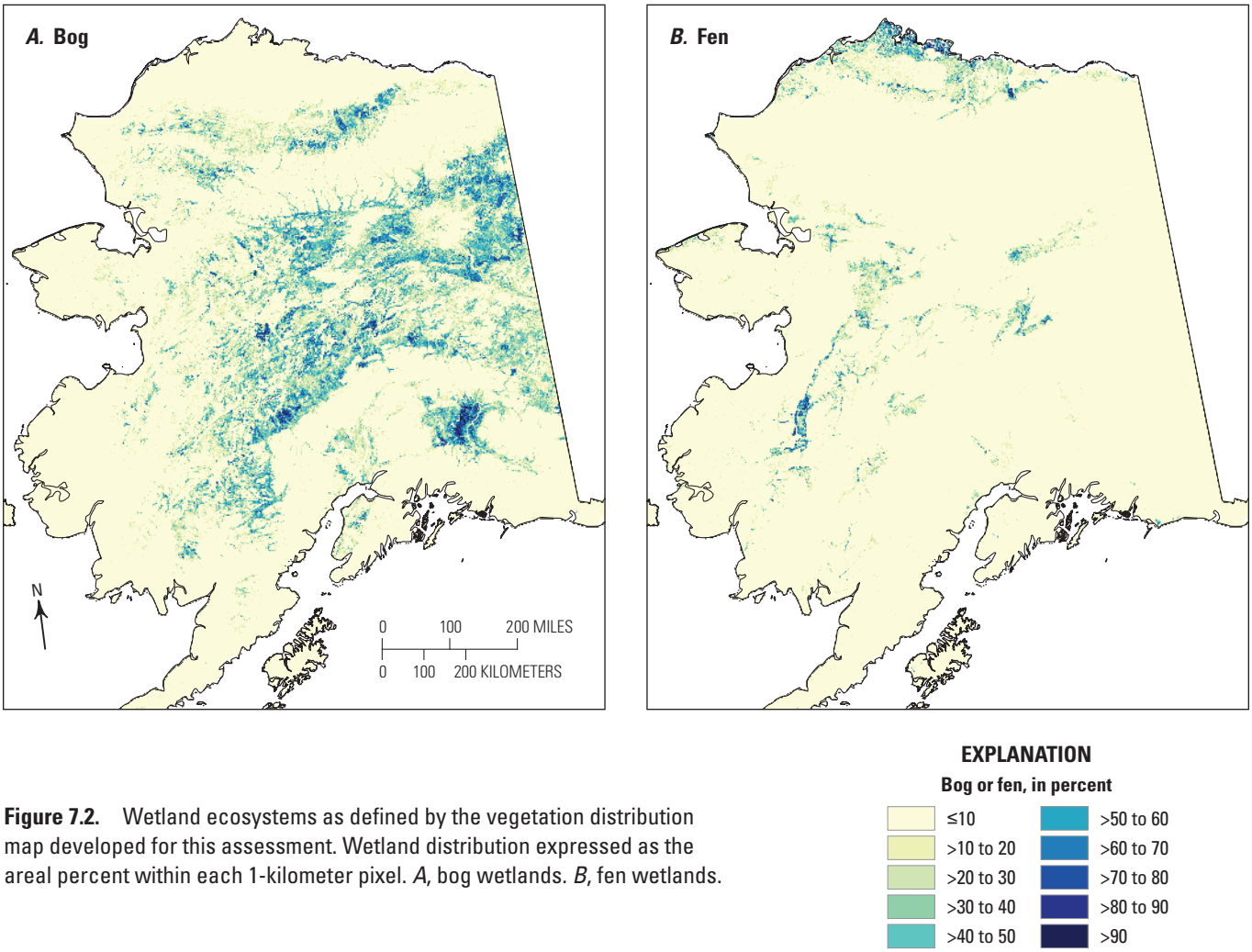

Figure 7.2. Wetland ecosystems as defined by the vegetation distribution map developed for this assessment. Wetland distribution expressed as the areal percent within each 1-kilometer pixel. *A*, bog wetlands. *B*, fen wetlands.

67 percent for the cross-validation (table 7.5). Fens tended to be classed more reliably than bogs, likely because woody overstory vegetation masked bog characteristics. Nonparametric techniques are sensitive to class frequency distributions so the number of pixels per class (bog, fen, other) is representative of the population being mapped.

The original 30-m maps of probable bog and fen distribution were converted to two maps of percent bog and percent fen at a 1-km resolution to match the resolution of the simulations (fig. 7.2).

7.4.2. Scaling Simulation Results for the Alternative Map of Wetland Distribution

Simulations of wetland distribution were conducted for the wetland ecosystems throughout Alaska at 1-km resolution. The estimates for a particular 1-km grid cell were then area-weighted by the wetland fraction for that 1-km grid cell provided by the wetland distribution map. The area-weighted estimates were then aggregated to the scale of LCC regions or to the scale of Alaska for purposes of analysis and reporting.

Table 7.3. Potential spatial input variables and those winnowed and subsequently mapped using a regression tree model.

[X, variable part of winnowed subset; —, variable not part of winnowed subset; ?, unknown; NA, not applicable]

Potential spatial input variables	Winnowed subset of variables	Variable usage by regression tree model (percent)	Reference
Web-enabled Landsat Data band 1	X	32	Roy and others (2010)
Web-enabled Landsat Data band 2	X	71	Roy and others (2010)
Web-enabled Landsat Data band 3	X	95	Roy and others (2010)
Web-enabled Landsat Data band 4	X	91	Roy and others (2010)
Web-enabled Landsat Data band 5	X	?	Roy and others (2010)
Web-enabled Landsat Data band 6	X	49	Roy and others (2010)
Web-enabled Landsat Data band 7	X	100	Roy and others (2010)
EVI (enhanced vegetation index)	—	—	Ji and others (2014)
gNDVI (green normalized difference vegetation index)	X	68	Ji and others (2014)
NDVI (normalized difference vegetation index)	—	—	Ji and others (2014)
SAVI (soil-adjusted vegetation index)	X	85	Ji and others (2014)
NDII (normalized difference infrared index)	—	—	Ji and others (2011)
NDII7 (normalized difference infrared index using band 7)	X	57	Ji and others (2011)
NDWI (normalized difference water index)	X	47	Ji and others (2011)
NDWI7 (normalized difference water index using band 7)	X	53	Ji and others (2011)
Sum of bands 4, 5, and 6	X	80	NA
Elevation	X	100	Gesch and others (2002)
Slope, in degrees	X	97	NA
Compound terrain index	X	47	Lu (2008)
Radar-based wetlands	X	32	Whitcomb and others (2009)
National Land Cover Database	X	87	Homer and others (2004)
China 2000	X	47	Liao and others (2014)
Soil texture	X	71	Jorgenson, Yoshikawa, and others (2008a)

Table 7.4. Accuracy assessments for the mapping model used to estimate bog and fen distribution compared with Alaska National Wetlands Inventory (NWI) reference classes for fens and bogs based on an independent test of 1,030 randomly selected pixels from the Alaska wetland distribution map developed for this assessment.

[NA, not applicable]

NWI reference	Mapping model				
	Bog	Fen	Other	Sum	Percent agreement
Bog	52	3	64	119	44
Fen	7	188	124	319	59
Other	42	18	532	592	90
Sum	101	209	720	1,030	NA
Percent	52	90	74	NA	75

Table 7.5. Accuracy assessments for the mapping model used to estimate bog and fen distribution compared with Alaska National Wetlands Inventory (NWI) reference classes for fens and bogs based on cross-validation of the pixels from the Alaska wetland distribution map developed for this assessment, not including those withheld for the independent test.

[NA, not applicable]

NWI reference	Mapping model				
	Bog	Fen	Other	Sum	Percent agreement
Bog	1,385	60	1,807	3,252	43
Fen	118	2,077	1,705	3,900	53
Other	985	956	7,901	9,842	80
Sum	2,488	3,093	11,413	16,994	NA
Percent	56	67	69	NA	67

7.4.3. Net Ecosystem Carbon Balance and Ecosystem Carbon Source/Sink Potential

Vegetation carbon stock estimates consisted of the sum of the aboveground and belowground living biomass. Soil carbon stocks consisted of the sum of carbon stored in the dead woody debris fallen to the ground, moss and litter, organic soil layers, and mineral soil layers. Historical changes in soil and vegetation carbon stocks were evaluated by quantifying annual differences of decadal averages between the first decade (1950–1959) and the last decade (2000–2009) of the historical period. Projected changes in soil and vegetation carbon stocks were evaluated by quantifying annual differences of decadal averages between the last decade of the historical period (2000–2009) and the last decade of the projection period (2090–2099).

The net ecosystem carbon balance (NECB) is the difference between total carbon inputs and total carbon outputs to the ecosystem (Chapin and others, 2006). NECB is the sum of all carbon fluxes coming in and out of the ecosystems, through gaseous and nongaseous, dissolved and nondissolved exchanges with the atmosphere and the hydrologic network. In terrestrial wetland ecosystems, NECB is the result of net primary productivity (NPP, net CO_2 uptake by the vegetation) minus heterotrophic respiration (HR), biogenic methane exchange ($BioCH_4$), and fire emissions (Fire). No export of carbon from forest harvest activities (Harvest) was expected in wetlands. No methane consumption was expected in wetlands for the anaerobic conditions are not favorable to methanotrophs activities. Furthermore, logging activities do not take place in lowlands because of limited accessibility and low productivity of forested lowland ecosystems.

$$NECB = NPP - HR - Fire - Harvest - BioCH_4 \quad (7.1)$$

NPP results from carbon assimilation from vegetation photosynthesis minus the respiration of the primary producers (autotrophic respiration). $BioCH_4$ results from the activity of methanogens and methanotrophs under anaerobic conditions. HR results from the decomposition of unfrozen soil organic carbon. Fire emissions encompass CO_2, CH_4, and carbon monoxide (CO) emissions. For the analysis of the inter-annual variations in sections 7.5.1.2 and 7.5.2.1, carbon fluxes were expressed in grams of carbon per square meter per year ($gC/m^2/yr$). For the regional assessments in sections 7.5.1.4 and 7.5.2.3, carbon fluxes were summed across the regions and expressed in teragrams of carbon per year (TgC/yr). Positive NECB indicates a gain of carbon to the ecosystem from the atmosphere, and negative NECB indicates a loss of carbon from the ecosystem to the atmosphere.

The uncertainty of carbon dynamics projected through the 21st century associated with climate forcing was estimated spatially by computing the range of change in NECB among the six climate simulations. For every 1-km grid cell and every climate simulation, the annual change in NECB was computed as the difference in the mean decadal NECB centered on 2095 and 2005 divided by the length of this period:

$$\Delta NECB = \frac{(NECB_{[2090-2099]} - NECB_{[2000-2009]})}{90} \quad (7.2)$$

The uncertainty was computed as the difference between the maximum and minimum ΔNECB among the six climate simulations.

Global warming potential (GWP) across time and the landscape was estimated taking into account that CH_4 has 25 times the GWP of CO_2 over a 100-year timeframe (Forster and others, 2007). GWP was reported in CO_2 equivalent by multiplying C-CH_4 fluxes by 33.33 (see chapter 6, section 6.3.5.2 for details). All C-CO_2 fluxes were converted to CO_2 equivalent by multiplying them by 3.66. CH_4 production from fire emissions ($Fire_{(CH4)}$) was considered in addition to biogenic CH_4 emissions by applying emission factors to CO_2, CH_4, and CO on DOS-TEM simulations of fire emissions (French and others, 2002). The carbon in CO was considered CO_2 because it converts to CO_2 in the atmosphere within a year (Weinstock, 1969).

$$GWP = -44/12 \times (NPP - HR - Harvest - Fire_{(CO2+CO)}) + 25 \times 16/12 \times (Fire_{(CH4)} + BioCH_4) \quad (7.3)$$

Positive GWP indicates a net loss of CO_2 from the ecosystem to the atmosphere, and negative GWP indicates a net gain of CO_2 to the ecosystem from the atmosphere.

Analysis of the time series was conducted using linear regression and the Fisher test for test of significance on the time series. For the analysis of the inter-annual variations in sections 7.5.1.2 and 7.5.2.1, carbon fluxes were expressed in $gC/m^2/yr$ with associated standard deviation (s.d.). For the regional assessments in sections 7.5.1.4 and 7.5.2.3., carbon fluxes were summed across the regions and expressed in TgC/yr. The assumptions of normality and homoscedasticity were verified by examining residual plots. The relative effects of temperature, precipitation, total area burned, and atmospheric CO_2 concentration on the carbon fluxes were tested using multiple regression analysis. The effects were considered significant when the p-value is lower than 0.05.

7.5. Results and Discussion

7.5.1. Historical Assessment of Carbon Dynamics (1950–2009)

7.5.1.1. Model Validation and Verification

For the historical period of the simulations (1950–2009), soil and vegetation carbon stocks were validated when possible by comparing modeled and observed estimates at sites independent from the sites used for model parameterization. When independent data (that is, data collected outside of the sites used for model parameterization) were not available, a verification of modeled versus observed stocks was conducted on the same sites used for model parameterization.

Globally, no significant differences were observed between modeled and observed contemporary vegetation carbon stocks (table 7.6; $p=0.340$) and soil carbon stocks (table 7.7; $p=0.182$). In general, DOS-TEM simulations successfully reproduced differences between land-cover types. Graminoid and wet-sedge tundra and maritime fen presented the lowest vegetation carbon stocks (table 7.3). Boreal lowland forests (that is, deciduous, white spruce, and black spruce lowland forests) had intermediate vegetation carbon stocks, and maritime wetland forest presented the largest vegetation carbon stocks, with 13.6 kilograms of carbon per square meter (kgC/m^2) observed.

In contrast, arctic and alpine tundra wetlands and maritime wetlands contained larger soil carbon stocks than boreal forest ecosystems (table 7.7).

Table 7.6. Comparison of observed and modeled vegetation carbon stocks for the main wetland land-cover types in Alaska.

[kgC/m^2, kilogram of carbon per square meter; NA, not applicable]

Wetland land-cover type	Number of sites used for model testing	Vegetation carbon stocks (kgC/m^2)			
		Mean		Standard deviation	
		Observed	Modeled	Observed	Modeled
Black spruce forest	45	2.47	1.99	0.85	0.38
White spruce forest	20	4.40	4.29	0.74	0.32
Deciduous forest	24	6.85	6.56	0.46	0.85
Graminoid tundra	3	0.56	0.44	0.26	0.21
Wet-sedge tundra	2	0.46	0.83	0.17	0.32
Maritime wetland forest[1]	3	13.62	13.11	1.16	3.26
Maritime fen[1]	1	0.96	1.67	NA	NA

[1]Comparisons between observed and modeled vegetation carbon stocks have been conducted for parameterization (that is, verification).

Table 7.7. Comparison of observed and modeled soil carbon stocks for the main wetland land-cover types in Alaska.

[kgC/m^2, kilogram of carbon per square meter; NA, not applicable]

Wetland land-cover type	Number of sites	Soil carbon stocks (kgC/m^2)			
		Mean		Standard deviation	
		Observed	Modeled	Observed	Modeled
Black spruce forest	22	29.85	46.84	11.15	55.64
White spruce forest	14	23.05	25.18	9.61	54.08
Deciduous forest	8	23.87	22.10	12.96	29.83
Tussock tundra	11	62.53	65.44	20.83	49.59
Wet-sedge tundra	23	42.01	50.73	30.49	31.46
Maritime wetland forest[1]	1	40.71	32.83	NA	NA
Maritime fen[1]	1	61.78	75.87	NA	NA

[1]Comparisons between observed and modeled vegetation carbon stocks have been conducted for parameterization (that is, verification).

7.5.1.2. Time Series Biogenic Methane Emissions, Net Ecosystem Carbon Balance, and Global Warming Potential for Wetland Alaska

For the wetland distribution map, the MDM-TEM simulation estimated net biogenic CH_4 emissions of wetlands in Alaska over the historical period (1950–2009) to be 157 grams of carbon dioxide equivalent per square meter per year (gCO_2-eq/m^2/yr) (s.d. of about 33 gCO_2-eq/m^2/yr), ranging from 97 to 267 gCO_2-eq/m^2/yr (fig. 7.3*A*). Biogenic CH_4 emissions increased significantly during the historical period, at a rate of about 0.977 gCO_2-eq/m^2/yr (Fisher value, $F=20.56$, $p<0.01$). Pyrogenic CH_4 emissions were estimated to be 1.50 gCO_2-eq/m^2/yr, which represented about 1 percent of the biogenic emissions. Pyrogenic CH_4 emissions significantly increased over the historical period ($F=2.13$, $p=0.0383$) at a rate of 0.037 gCO_2-eq/m^2/yr. NECB was estimated at –12.6 gC/m^2/yr (s.d. 7.2 gC/m^2/yr), ranging from –313.3 to 50.5 gC/m^2/yr. NECB did not change significantly over the historical period ($F=0.22$, $p=0.63$, fig. 7.3*B*). The GWP over the historical period indicated that wetlands were a significant source of greenhouse gas forcing of 187.7 gCO_2-eq/m^2/yr (s.d. 112.4 gCO_2-eq/m^2/yr), ranging from 57.4 to 1,399 gCO_2-eq/m^2/yr. GWP did not change significantly over the historical period ($F=0.87$, $p=0.35$, fig. 7.3*C*) and was significantly different from zero ($t=-6.00$; $p<0.01$).

7.5.1.3. Environmental Drivers of the Historical Temporal Variability of Biogenic Methane Emissions, Net Ecosystem Carbon Balance, and Global Warming Potential of Wetland Alaska

Total CH_4 emissions (biogenic and pyrogenic) during the historical period were positively correlated with the annual area of wetlands burned associated with peaks of pyrogenic methane emissions. CH_4 emissions increased with increasing atmospheric CO_2 concentration (table 7.8). The positive relationship between atmospheric CO_2 concentration and CH_4 emissions is likely related to the effect of increasing atmospheric CO_2 on NPP (see chapter 6, section 6.4.2.2). The negative effect of annual area burned on NECB is related to the effect of wildfire on CO_2 emissions from combustion of soil and vegetation carbon. Although GWP is positively correlated with annual area burned, the relationship likely depends on the correlation of GWP and CH_4 emissions.

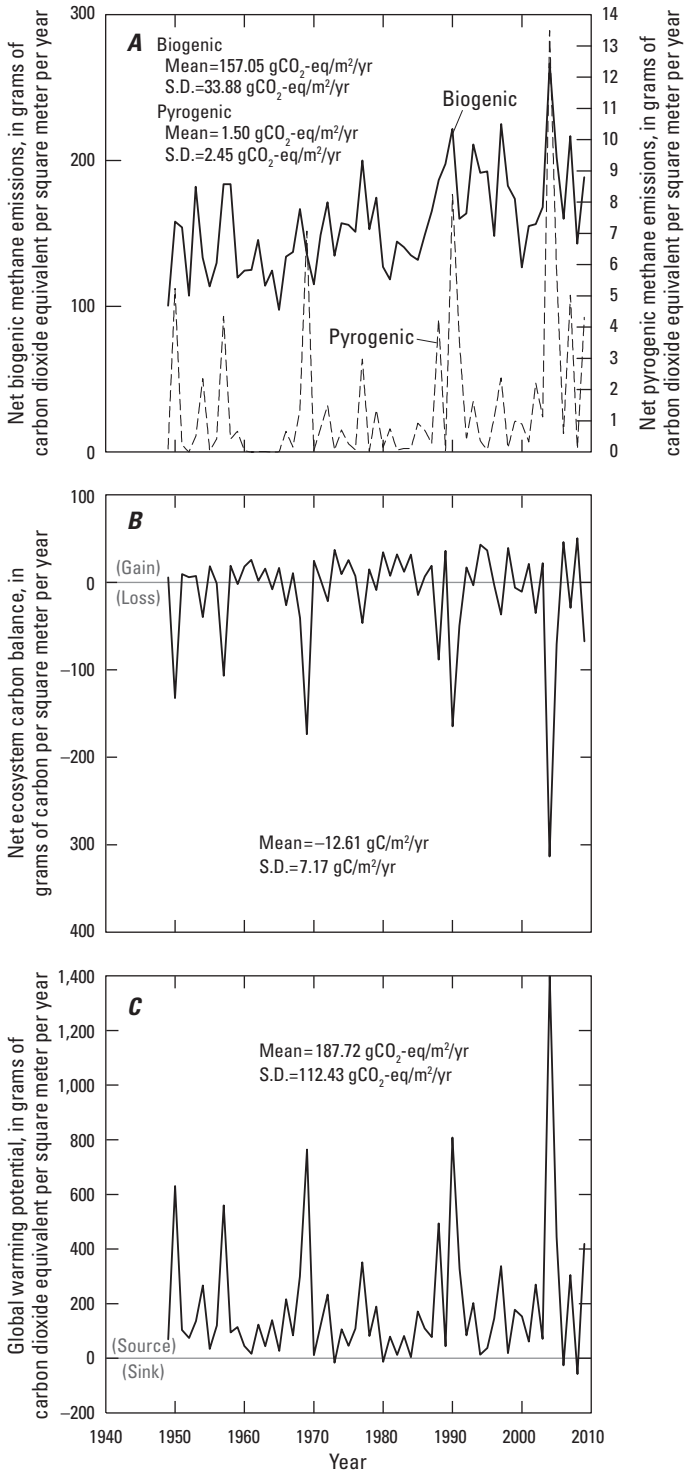

Figure 7.3. Time series of annual *A*, net biogenic and pyrogenic methane emissions; *B*, net ecosystem carbon balance; and *C*, global warming potential during the historical period (1950–2009) for wetland ecosystems of Alaska defined by the wetland distribution map. The mean and standard deviation for the study area are indicated in each panel.

7.5.1.4. Spatial Distribution of Carbon Stocks, Biogenic Methane Emissions, Net Ecosystem Carbon Balance, and Global Warming Potential Across Wetland Alaska

The largest carbon stocks of wetlands in Alaska were located in the Northwest Boreal LCC North (table 7.9), with storage of 427 teragrams of carbon (TgC) in the vegetation and 1,965 TgC in the soil. The Northwest Boreal LCC North also contains the largest proportion of wetlands in Alaska and is the only LCC region in which carbon stocks in the vegetation and the soil decreased during the historical period. The largest increase of carbon stocks in the vegetation and the soil was observed in the Arctic LCC, with a gain of 0.12 TgC/yr and 0.49 TgC/yr in the vegetation and the soil, respectively.

During the first decade of the 21st century (2000–2009), the largest biogenic CH_4 emissions were observed in the Northwest Boreal LCC North (table 7.10, fig. 7.4*A*). The largest NPP also was observed in the Northwest Boreal LCC North but the carbon gain from vegetation growth was offset by carbon loss from heterotrophic respiration and fire emissions, resulting in the wetlands in the region being a net carbon source of –2.21 TgC/yr during the historical period (fig. 7.4*B*), equivalent to 27 teragrams of carbon dioxide equivalent per year ($TgCO_2$-eq/yr) (fig. 7.4*C*). The other LCC regions were carbon sinks during the historical period: the largest sink was located in the Arctic LCC with storage of 0.62 TgC/yr. However, these smaller sinks were not large enough to compensate for the carbon loss from the Northwest Boreal LCC North. Statewide, wetland ecosystems in Alaska were a carbon source during the historical period, losing about 1.34 TgC/yr. The carbon losses were about equally distributed among soil and vegetation (table 7.9). Although total CH_4 emissions represented only 2.6 percent of NPP, the trend of GWP is dominated by CH_4 emissions. As a result, mean annual GWP between 2000 and 2009 was 33 $TgCO_2$-eq/yr in wetlands of Alaska.

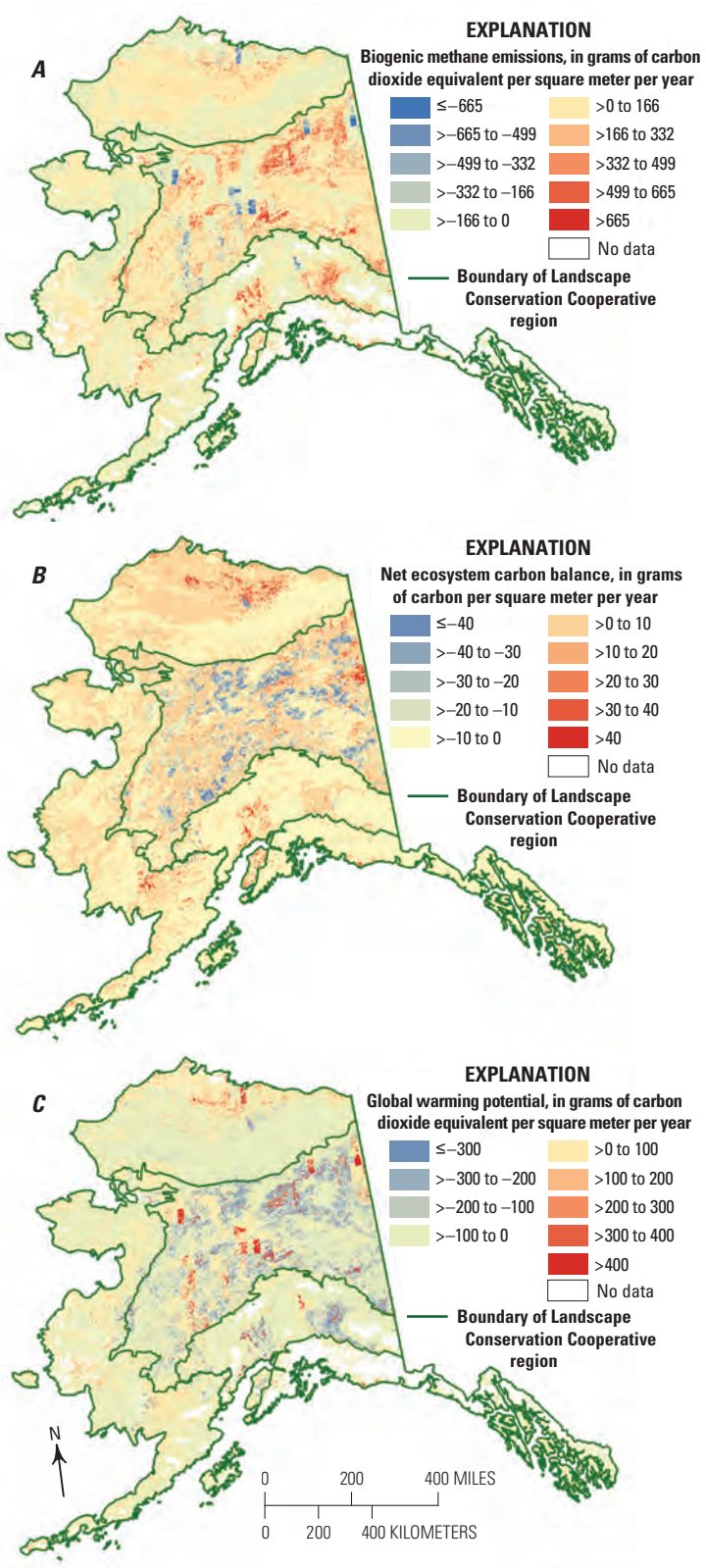

Figure 7.4. Spatial distribution of mean annual *A*, biogenic methane emissions; *B*, net ecosystem carbon balance; and *C*, global warming potential for the historical period (1950–2009) for wetland ecosystems of Alaska.

Table 7.8. Results of multiple linear regressions testing the main drivers of carbon dioxide and total methane (biogenic and pyrogenic) fluxes in wetland ecosystems among total annual precipitation, mean annual temperature, annual area burned, and mean annual atmospheric carbon dioxide concentration during the historical period (1950–2009).

[F, Fisher value; P, probability value. Trend: +, positive; –, negative; n.s., trend not significant. Units: mm, milllimeter; °C, degree Celsius; km^2, square kilometer; ppm, part per million. CO_2, carbon dioxide]

Drivers of carbon dioxide and methane fluxes	Total methane emissions			Net ecosystem carbon balance			Global warming potential		
	F	P	Trend	F	P	Trend	F	P	Trend
Total annual precipitation (mm)	0.01	0.92	n.s.	0.55	0.46	n.s.	0.41	0.52	n.s.
Mean annual temperature (°C)	1.75	0.19	n.s.	0.44	0.51	n.s.	0.02	0.88	n.s.
Annual area burned (km^2)	29.3	<0.01	+	217.77	<0.01	–	221.36	<0.01	+
Mean annual atmospheric CO_2 concentration (ppm)	5.13	<0.01	+	1.07	0.31	n.s.	0.55	0.46	n.s.

Table 7.9. Average vegetation and soil carbon stocks for the last decade of the historical period (2000–2009) and mean annual change in vegetation and soil carbon stocks between the first (1950–1959) and last (2000–2009) decades of the historical period in each Landscape Conservation Cooperative region for wetland ecosystems of Alaska defined by the vegetation distribution map developed for this assessment.

[Data may not add to totals shown because of independent rounding. km^2, square kilometer; TgC, teragram of carbon]

Landscape Conservation Cooperative (LCC) region	Wetland total area (km^2)	Wetland cover (percent)	Vegetation carbon stocks (TgC)		Soil carbon stocks (TgC)	
			Average	Mean annual change	Average	Mean annual change
Arctic LCC	29,818	9.8	44	0.12	1,281	0.49
Western Alaska LCC	14,582	3.9	57	0.04	788	0.06
Northwest Boreal LCC North	112,077	24.5	427	–0.87	1,965	–1.33
Northwest Boreal LCC South	18,627	10.0	83	0.05	865	0.03
North Pacific LCC	1,965	1.3	19	0.00	107	0.06
Total	**177,069**	**12.0**	**630**	**–0.65**	**5,006**	**–0.68**

Table 7.10. Average vegetation and soil carbon fluxes in wetland ecosystems per Landscape Conservation Cooperative region from 2000 through 2009.

[Data may not add to totals or compute to net ecosystem carbon balance shown because of independent rounding. CO_2, carbon dioxide; CO, carbon monoxide; CH_4, methane; TgC/yr, teragram of carbon per year; $TgCO_2$-eq/yr, teragram of carbon dioxide equivalent per year]

Landscape Conservation Cooperative (LCC) region	Pyrogenic CO_2 + CO emissions (TgC/yr)	Pyrogenic CH_4 emissions ($TgCO_2$-eq/yr)	Net primary productivity (TgC/yr)	Biogenic CH_4 emissions ($TgCO_2$-eq/yr)	Heterotrophic respiration (TgC/yr)	Net ecosystem carbon balance (TgC/yr)	Global warming potential ($TgCO_2$-eq/yr)
Arctic LCC	1.08	0.112	4.68	2.49	2.91	0.62	0.06
Western Alaska LCC	0.08	0.008	2.99	1.67	2.76	0.10	1.12
Northwest Boreal LCC North	8.23	0.740	24.95	20.45	18.29	–2.21	27.01
Northwest Boreal LCC South	1.00	0.105	4.11	5.74	2.85	0.08	4.90
North Pacific LCC	0.01	0.001	0.56	0.50	0.47	0.07	0.20
Total	**10.40**	**0.966**	**37.28**	**30.85**	**27.27**	**–1.34**	**33.30**

7.5.2. Future Assessment of Carbon Dynamics (2010–2099)

7.5.2.1. Times Series for Wetland Alaska

Estimates of future biogenic CH_4 emissions exhibited substantial inter-annual variability and substantial differences between climate models for a given emissions scenario and among different emissions scenarios for a given climate model. The greatest mean annual biogenic CH_4 emissions among climate models and emissions scenarios would be about 229 gCO_2-eq/m^2/yr under scenario A1B with ECHAM5. The lowest mean annual biogenic CH_4 emissions were projected under scenario B1 with both climate models (159 gCO_2-eq/m^2/yr and 176 gCO_2-eq/m^2/yr with CGCM3.1 and ECHAM5, respectively; fig. 7.5*A*). Biogenic CH_4 emissions would increase significantly during the 21st century under scenarios B1, A1B, and A2 at a rate of 0.680 gCO_2-eq/m^2/yr, 1.406 gCO_2-eq/m^2/yr, and 3.073 gCO_2-eq/m^2/yr, respectively, with CGCM3.1 and 0.923 gCO_2-eq/m^2/yr, 1.003 gCO_2-eq/m^2/yr, and 2.183 gCO_2-eq/m^2/yr, respectively, with ECHAM5.

Projected mean annual pyrogenic CH_4 emissions were larger for the climate simulations from the ECHAM5 climate model than from the CGCM3.1 climate model (fig. 7.5*B*). Among all climate simulations, mean annual pyrogenic CH_4 emissions would range from 0.967 gCO_2-eq/m^2/yr (s.d. 1.3 gCO_2-eq/m^2/yr) under scenario A1B with CGCM3.1 to 1.467 gCO_2-eq/m^2/yr (s.d. 2.7 gCO_2-eq/m^2/yr) under scenario A2 with ECHAM5. Pyrogenic CH_4 emissions are not projected to significantly increase over time, except for the climate simulations with the largest warming and increase in atmospheric CO_2 concentration (that is, scenario A2 with CGCM3.1 and ECHAM5), for which pyrogenic CH_4 emissions would increase at a rate of 0.00243 gCO_2-eq/m^2/yr and 0.0193 gCO_2-eq/m^2/yr, respectively. Combining historical simulation results, CH_4 emissions significantly increased from 1950 through 2009 by 0.967 gCO_2-eq/m^2/yr.

For each climate model, projected mean annual NECB was the lowest for the lowest CO_2-emissions scenario B1 (13.8 gC/m^2/yr and 23.5 gC/m^2/yr with CGCM3.1 and ECHAM5, respectively) and the highest for the highest CO_2-emissions scenario A2 (33.6 gC/m^2/yr and 31.7 gC/m^2/yr with CGCM3.1 and ECHAM5, respectively). In contrast with CH_4 emissions, NECB would not change significantly over time (fig. 7.5*C*). As a result, GWP was projected to increase during the second half of the 21st century (fig. 7.5*D*). This increase was significant for CGCM3.1 climate simulations under A2 and B1 emissions scenarios (rate of 2.59 gCO_2-eq/m^2/yr and 1.09 gCO_2-eq/m^2/yr, respectively) and the ECHAM5 climate simulation under the A1B scenario (rate of 2.15 gCO_2-eq/m^2/yr).

7.5.2.2. Environmental Drivers of the Future Temporal Variability of Net Ecosystem Carbon Balance and Global Warming Potential in Wetland Alaska

Over the projection period, increasing annual area burned and rising atmospheric CO_2 concentrations were projected to be associated with an increase in CH_4 emissions in wetlands during the 21st century for all six climate simulations. Increasing air temperature also would have a significant positive effect on CH_4 emissions under scenarios A1B and A2 with CGCM3.1 (table 7.11). Increasing annual area burned would have a negative effect on NECB for all climate simulations. Increasing air temperature and atmospheric CO_2 concentration also would have a positive effect on NECB for scenarios B1 and A1B, respectively, with ECHAM5. Increases in GWP would be associated with increases in annual area burned owing to climate warming (see chapter 2, section 2.4.5.2.). For all simulations, fire regime would therefore be the main driver of the carbon balance in wetlands during the 21st century. However, the present assessment does not take into account the effect environmental changes associated with thermokarst formation have on the carbon balance. Permafrost in wetlands of Alaska is often ice rich (Jorgenson, Shur, and others, 2008). With increasing temperature and permafrost thaw, the soil of ice-rich wetlands can collapse as a result of ice melting to water and draining out of the ecosystem (Jorgenson, Yoshikawa, and others, 2008b). These collapses are associated with drastic changes in hydrology—transitioning from moist permafrost plateau to saturated drainage conditions—and important changes in the vegetation composition (from permafrost plateau forest to bog or fen, for instance) (Jorgenson and Osterkamp, 2005). Thermokarsts can be triggered by climate and fire (Myers-Smith and others, 2008). The transition from moist to saturated conditions may considerably affect the local carbon balance, increasing not only CH_4 production (Turetsky and others, 2008) but also soil carbon storage (O'Donnell and others, 2012). However, the extent of thermokarst across Alaska is still unknown. Therefore, it is difficult to assess the effect of thermokarst disturbance on the regional carbon balance of Alaska.

Table 7.11. Results of multiple linear regressions testing the main drivers of carbon dioxide and methane fluxes in wetland ecosystems among total annual precipitation, mean annual temperature, annual area burned, and mean annual atmospheric carbon dioxide concentration for each future climate simulation for the projection period (2010–2099).

[The six future climate simulations are combinations of two general circulation models, version 3.1-T47 of the Coupled Global Climate Model (CGCM3.1) developed by the Canadian Centre for Climate Modelling and Analysis and version 5 of the European Centre Hamburg Model (ECHAM5) developed by the Max Planck Institute, and three climate scenarios of the Intergovernmental Panel on Climate Change's Special Report on Emissions Scenarios (Nakićenović and Swart, 2000), B1, A1B, and A2, in order of low to high projected CO_2 emissions. F, Fisher value; P, probability value. Trend: +, positive; –, negative; n.s., trend not significant. Units: mm, milllimeter; °C, degree Celsius; km^2, square kilometer; ppm, part per million. CO_2, carbon dioxide]

Climate scenario	Parameter	Total methane emissions			Net ecosystem carbon balance			Global warming potential		
		F	P	Trend	F	P	Trend	F	P	Trend
CGCM3.1										
A1B	Total annual precipitation (mm)	0.01	0.92	n.s.	0.1	0.75	n.s.	0.1	0.75	n.s.
	Mean annual temperature (°C)	5.79	0.02	+	3	0.09	n.s.	0.21	0.65	n.s.
	Annual area burned (km^2)	7.04	0.01	+	78.6	<0.01	–	79.63	<0.01	+
	Mean annual atmospheric CO_2 concentration (ppm)	4.42	0.04	+	0.03	0.87	n.s.	0.61	0.44	n.s.
A2	Total annual precipitation (mm)	0.01	0.92	n.s.	0.1	0.75	n.s.	0.1	0.75	n.s.
	Mean annual temperature (°C)	5.79	0.02	+	3	0.09	n.s.	0.21	0.65	n.s.
	Annual area burned (km^2)	7.04	0.01	+	78.6	<0.01	–	79.63	<0.01	+
	Mean annual atmospheric CO_2 concentration (ppm)	4.42	0.04	+	0.03	0.87	n.s.	0.61	0.44	n.s.
B1	Total annual precipitation (mm)	0	0.98	n.s.	0.58	0.45	n.s.	0.46	0.50	n.s.
	Mean annual temperature (°C)	1.49	0.23	n.s.	0.52	0.47	n.s.	0.05	0.82	n.s.
	Annual area burned (km^2)	17.87	<0.01	+	109.52	<0.01	–	119.76	<0.01	+
	Mean annual atmospheric CO_2 concentration (ppm)	4.89	0.03	+	0.17	0.68	n.s.	0.15	0.70	n.s.
ECHAM5										
A1B	Total annual precipitation (mm)	1.78	0.19	n.s.	2.2	0.14	n.s.	3.48	0.07	n.s.
	Mean annual temperature (°C)	0.14	0.71	n.s.	1.64	0.20	n.s.	1.04	0.31	n.s.
	Annual area burned (km^2)	19.61	<0.01	+	169.32	<0.01	–	117.55	<0.01	+
	Mean annual atmospheric CO_2 concentration (ppm)	11.67	<0.01	+	5.86	0.02	+	1.45	0.23	n.s.
A2	Total annual precipitation (mm)	0.47	0.49	n.s.	2.48	0.12	n.s.	2.16	0.15	n.s.
	Mean annual temperature (°C)	9.27	<0.01	+	0.07	0.80	n.s.	2.39	0.13	n.s.
	Annual area burned (km^2)	14.22	<0.01	+	136.49	<0.01	–	106.3	<0.01	+
	Mean annual atmospheric CO_2 concentration (ppm)	0.53	0.47	n.s.	1.27	0.26	n.s.	0.26	0.61	n.s.
B1	Total annual precipitation (mm)	0.97	0.33	n.s.	0.05	0.83	n.s.	0.61	0.44	n.s.
	Mean annual temperature (°C)	0.88	0.35	n.s.	5.03	0.03	+	1.76	0.19	n.s.
	Annual area burned (km^2)	19.03	<0.01	+	150.02	<0.01	–	168.94	<0.01	+
	Mean annual atmospheric CO_2 concentration (ppm)	4.33	0.04	+	0.52	0.47	n.s.	3.49	0.07	n.s.

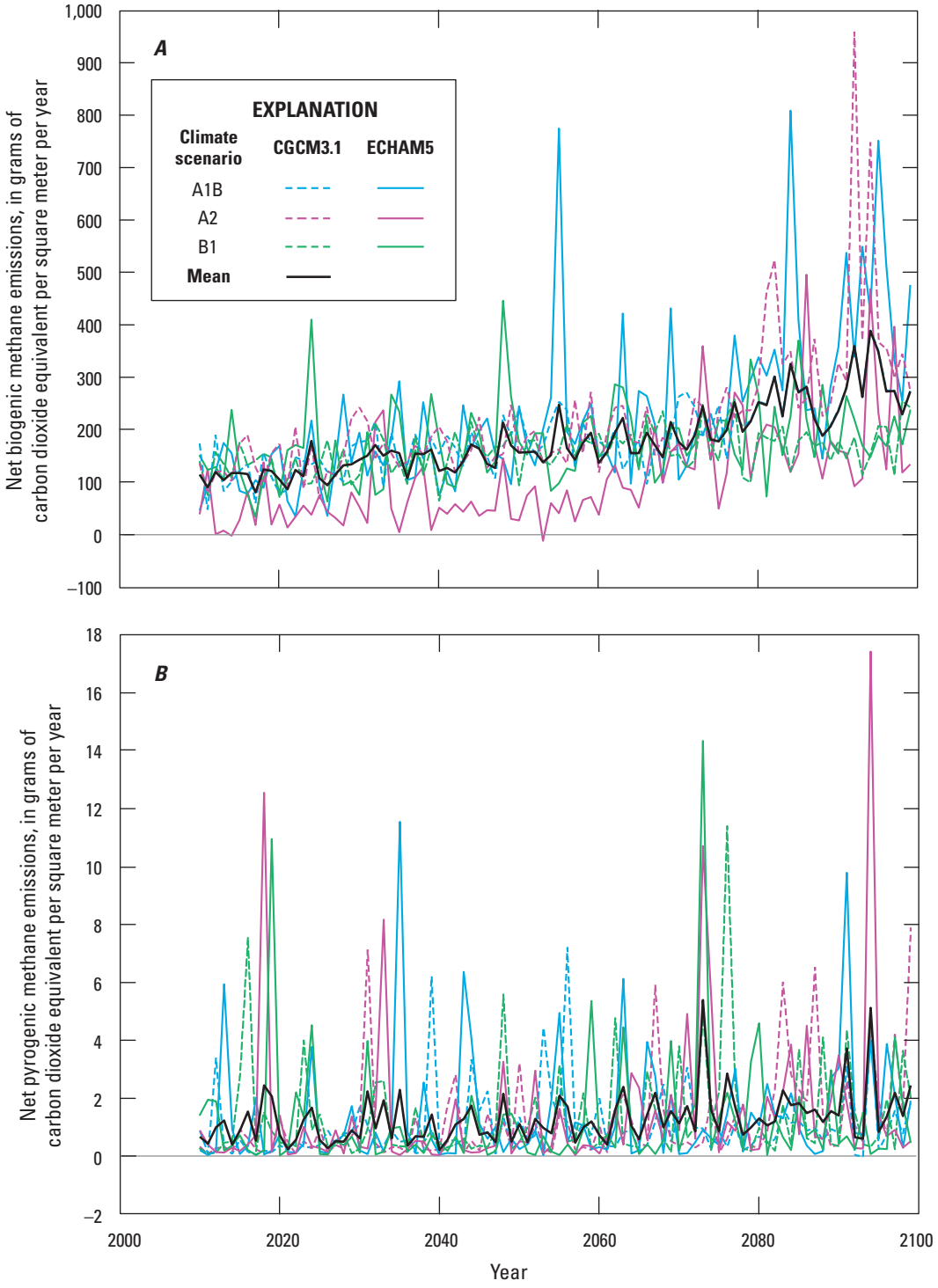

Figure 7.5. (pages 148 and 149). Time series of projected annual *A*, net biogenic methane emissions; *B*, net pyrogenic methane emissions; *C*, net ecosystem carbon balance; and *D*, global warming potential for the projection period (2010–2099) for wetland ecosystems of Alaska defined by the wetland distribution map for the two general circulation models, version 3.1-T47 of the Coupled Global Climate Model (CGCM3.1) developed by the Canadian Centre for Climate Modelling and Analysis and version 5 of the European Centre Hamburg Model (ECHAM5) developed by the Max Planck Institute, under three climate scenarios of the Intergovernmental Panel on Climate Change's Special Report on Emissions Scenarios (Nakićenović and Swart, 2000), B1, A1B, and A2, in order of low to high projected CO_2 emissions.

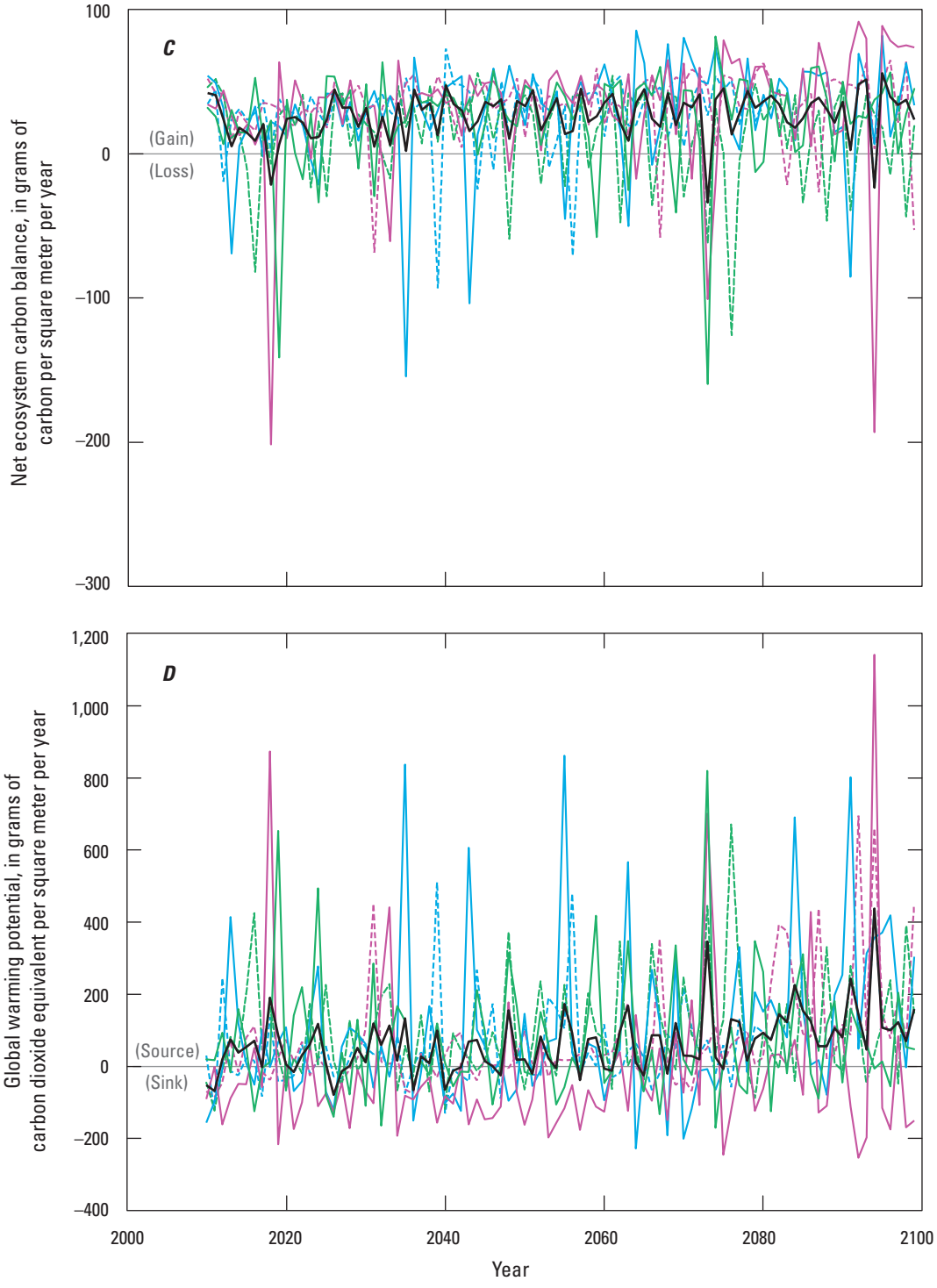

Figure 7.5.—Continued

7.5.2.3. Spatial Distribution of Changes in Carbon Stocks, Biogenic Methane Emissions, Net Ecosystem Carbon Balance, and Global Warming Potential Across Wetland Alaska

For each LCC region, the climate scenario associated with the largest increase in atmospheric CO_2 (that is, emissions scenario A2; table 7.12) induced the largest increase in vegetation and soil carbon stocks by 2099. Vegetation carbon stocks for the ECHAM5 climate simulations were generally projected to be higher than the vegetation carbon stocks for the CGCM3.1 climate simulations. In contrast, soil carbon stocks for the ECHAM5 climate simulations were generally projected to be lower than for the CGCM3.1 climate simulations. These differences were related to the fact that the ECHAM5 simulations presented larger warming trends and larger fire activity than the climate simulations from CGCM3.1 (see chapter 2 for detailed comparison). Warmer temperatures from the ECHAM5 climate simulations induced larger vegetation productivity and biomass compared with the results from the CGCM3.1 simulations. However, the larger litterfall associated with larger vegetation productivity was offset by carbon loss from the higher heterotrophic respiration and larger carbon emissions from wildfire, leading to lower soil carbon stocks projected for the ECHAM5 climate simulations compared with the CGCM3.1 climate simulations. Vegetation and soil carbon stocks were projected to increase from 2010 to 2099 for all regions and all simulations, except for the B1 scenario with CGCM3.1 in the Northwest Boreal LCC South (vegetation carbon stocks only) and the Western Alaska LCC.

Vegetation productivity was generally projected to be higher for the ECHAM5 climate simulations than for the CGCM3.1 climate simulations, except for the North Pacific LCC (table 7.13). Similarly, NPP was projected to increase in response to the scenarios projecting a greater increase in atmospheric CO_2 (scenarios A1B and A2 versus scenario B1). Statewide, mean annual NPP was projected to range from 41.0 to 46.7 TgC/yr between 2090 and 2099.

Among all time periods, the North Pacific LCC remained the minimal contributor to CH_4 emissions owing to the small wetland fraction in that region. Similar to the regional total CH_4 emission, the inter-scenario difference in emission magnitude is generally greater than that between the two GCMs within a scenario (table 7.13), indicating the dominating effects of climate controls on regional CH_4 dynamics. By the end of the 21st century, biogenic and pyrogenic CH_4 emissions were projected to range from 36 to 90 $TgCO_2$-eq/yr with biogenic CH_4 emissions representing 98 to 99 percent of the total emissions.

Projected fire emissions tended to increase in response to warming in the LCC regions. These projected increases were often accompanied by lower projected heterotrophic respiration (compared with simulations with lower warming trends). For instance, in the Northwest Boreal LCC North, whereas fire emissions were projected to increase by 95 percent on average in the A2 simulations compared with the B1 simulations, heterotrophic respiration was projected to decrease by 5 percent (table 7.13). This decrease in heterotrophic respiration is likely caused by the loss of organic horizon carbon from wildfire.

Carbon stocks in wetland ecosystems of all LCC regions were projected to increase within all six future climate simulations. The projected increase in carbon storage for Alaska ranged from 3.01 to 5.28 TgC/yr between the CGCM3.1 climate simulations under scenarios B1 and A2, respectively. NECB was generally projected to be highest for the A2 climate simulations, which had the greatest projected increases in atmospheric CO_2 and warming. Because the projected fire activity for 2090–2099 was lower than during 2000–2009, the NECB of the LCC regions was generally projected to be higher compared with 2000–2009 (table 7.10), except for the Western Alaska LCC under the B1 scenario. However, GWP estimates for the future climates indicate that all LCC regions would become sources of greenhouse gas radiative forcing by the end of the 21st century, except for CGCM3.1 simulations under scenarios A1B and B1 for the Arctic and North Pacific LCCs and the ECHAM5 simulation under scenario A2 for the Arctic LCC.

The spatial distribution of changes in biogenic CH_4 emissions indicated that there are large areas of projected increases in CH_4 emissions across Alaska from 2000–2009 to 2090–2099 (fig. 7.6), especially in central Alaska (Northwest Boreal LCC). Projected increases in central Alaska ranged from 6.7 gCO_2-eq/m^2/yr for the B1 climates to 16.7 gCO_2-eq/m^2/yr for the A2 climates, primarily owing to relatively large vegetation biomass, leaf area index, and productivity, associated with higher CH_4 production.

The average projected increase of NECB from 2000–2009 to 2090–2099 was largest in the Northwest Boreal LCC North (fig. 7.7*A*). The largest variation across climate simulations in changes of the projected NECB was in the Western Alaska LCC and the Northwest Boreal LCC South (fig. 7.7*B*). These regions could therefore be major sources of uncertainty as to how NECB responds to future climate and disturbance regimes.

Table 7.12. Average vegetation and soil carbon stocks for the last decade of the projection period (2090–2099) and mean annual change in vegetation and soil carbon stocks between the last decades of the historical period (2000–2009) and the projection period (2090–2099) per Landscape Conservation Cooperative region for each of the six climate simulations.

[The six climate simulations are combinations of two general circulation models, version 3.1-T47 of the Coupled Global Climate Model (CGCM3.1) developed by the Canadian Centre for Climate Modelling and Analysis and version 5 of the European Centre Hamburg Model (ECHAM5) developed by the Max Planck Institute, and three climate scenarios of the Intergovernmental Panel on Climate Change's Special Report on Emissions Scenarios (Nakićenović and Swart, 2000), B1, A1B, and A2, in order of low to high projected CO_2 emissions. Data may not add to totals shown because of independent rounding. TgC, teragram of carbon]

Climate scenario	Landscape Conservation Cooperative (LCC) region	Vegetation carbon stocks (TgC)		Soil carbon stocks (TgC)	
		Average	Mean annual change	Average	Mean annual change
		CGCM3.1			
A1B	Arctic LCC	59	0.16	1,395	1.23
	Western Alaska LCC	61	0.04	861	0.28
	Northwest Boreal LCC North	546	1.32	2,039	0.70
	Northwest Boreal LCC South	83	0.00	823	0.33
	North Pacific LCC	23	0.04	129	0.09
Total		**771**	**1.57**	**5,248**	**2.64**
A2	Arctic LCC	58	0.15	1,365	0.94
	Western Alaska LCC	63	0.07	816	0.30
	Northwest Boreal LCC North	551	1.38	2,121	1.73
	Northwest Boreal LCC South	87	0.04	912	0.52
	North Pacific LCC	24	0.05	114	0.08
Total		**783**	**1.70**	**5,328**	**3.58**
B1	Arctic LCC	55	0.14	1,323	1.25
	Western Alaska LCC	56	–0.00	836	–0.16
	Northwest Boreal LCC North	512	0.95	2,003	0.46
	Northwest Boreal LCC South	83	–0.01	888	0.24
	North Pacific LCC	23	0.03	116	0.10
Total		**728**	**1.11**	**5,165**	**1.90**
		ECHAM5			
A1B	Arctic LCC	62	0.19	1,354	0.80
	Western Alaska LCC	66	0.10	787	0.03
	Northwest Boreal LCC North	578	1.69	2,074	1.18
	Northwest Boreal LCC South	86	0.04	807	0.27
	North Pacific LCC	24	0.05	124	0.04
Total		**815**	**2.07**	**5,146**	**2.32**
A2	Arctic LCC	62	0.20	1,359	0.90
	Western Alaska LCC	66	0.10	817	0.10
	Northwest Boreal LCC North	579	1.69	2,093	1.38
	Northwest Boreal LCC South	92	0.09	847	0.17
	North Pacific LCC	23	0.04	111	0.04
Total		**822**	**2.13**	**5,226**	**2.58**
B1	Arctic LCC	56	0.13	1,357	0.86
	Western Alaska LCC	64	0.08	796	–0.02
	Northwest Boreal LCC North	563	1.49	2,049	0.71
	Northwest Boreal LCC South	85	0.01	878	0.13
	North Pacific LCC	23	0.04	114	0.07
Total		**791**	**1.75**	**5,193**	**1.75**

Table 7.13. Average annual vegetation and soil carbon fluxes for the last decade of the projection period (2090–2099) per Landscape Conservation Cooperative region for each of the six future climate simulations.

[The six climate simulations are combinations of two general circulation models, version 3.1-T47 of the Coupled Global Climate Model (CGCM3.1) developed by the Canadian Centre for Climate Modelling and Analysis and version 5 of the European Centre Hamburg Model (ECHAM5) developed by the Max Planck Institute, and three climate scenarios of the Intergovernmental Panel on Climate Change's Special Report on Emissions Scenarios (Nakićenović and Swart, 2000), B1, A1B, and A2, in order of low to high projected CO_2 emissions. Data may not add to totals or compute to net ecosystem carbon balance shown because of independent rounding. CO_2, carbon dioxide; CO, carbon monoxide; CH_4, methane; TgC/yr, teragram of carbon per year; $TgCO_2$-eq/yr, teragram of carbon dioxide equivalent per year]

Climate scenario	Landscape Conservation Cooperative (LCC) region	Pyrogenic CO_2 + CO emissions (TgC/yr)	Pyrogenic CH_4 emissions ($TgCO_2$-eq/yr)	Net primary productivity (TgC/yr)	Biogenic CH_4 emissions ($TgCO_2$-eq/yr)	Heterotrophic respiration (TgC/yr)	Net ecosystem carbon balance (TgC/yr)	Global warming potential ($TgCO_2$-eq/yr)
				CGCM3.1				
A1B	Arctic LCC	0.00	0.00	6.16	2.63	4.68	1.40	–2.77
	Western Alaska LCC	0.50	0.05	3.48	1.98	2.59	0.32	0.63
	Northwest Boreal LCC North	2.65	0.24	28.20	24.36	22.79	2.02	14.55
	Northwest Boreal LCC South	0.45	0.04	4.36	6.66	3.38	0.33	4.76
	North Pacific LCC	0.01	0.00	0.68	0.49	0.52	0.13	–0.04
	Total	**3.61**	**0.34**	**42.87**	**36.13**	**33.96**	**4.20**	**17.13**
A2	Arctic LCC	2.86	0.30	6.86	4.29	2.77	1.09	0.10
	Western Alaska LCC	2.38	0.24	3.68	3.07	0.82	0.38	1.57
	Northwest Boreal LCC North	3.70	0.35	28.35	44.94	20.17	3.12	28.98
	Northwest Boreal LCC South	1.57	0.16	4.61	11.45	2.12	0.57	8.27
	North Pacific LCC	0.17	0.02	0.79	0.69	0.47	0.13	0.17
	Total	**10.68**	**1.06**	**44.29**	**64.44**	**26.36**	**5.28**	**39.09**
B1	Arctic LCC	0.00	0.00	6.18	2.57	4.71	1.39	–2.82
	Western Alaska LCC	1.33	0.13	3.30	1.85	2.07	–0.16	2.36
	Northwest Boreal LCC North	2.58	0.24	26.64	24.97	21.89	1.40	17.34
	Northwest Boreal LCC South	0.96	0.10	4.21	7.15	2.80	0.24	5.59
	North Pacific LCC	0.00	0.00	0.66	0.52	0.51	0.13	–0.01
	Total	**4.87**	**0.47**	**40.99**	**37.06**	**31.98**	**3.01**	**22.46**
				ECHAM5				
A1B	Arctic LCC	3.54	0.37	7.50	6.23	2.77	0.99	2.25
	Western Alaska LCC	2.16	0.22	3.82	3.95	1.40	0.13	3.23
	Northwest Boreal LCC North	3.81	0.35	29.02	61.48	20.49	2.87	44.65
	Northwest Boreal LCC South	1.84	0.18	4.68	15.72	2.05	0.31	13.05
	North Pacific LCC	0.20	0.02	0.78	1.28	0.44	0.09	0.83
	Total	**11.55**	**1.15**	**45.80**	**88.66**	**27.15**	**4.39**	**64.02**
A2	Arctic LCC	3.59	0.37	7.51	3.32	2.72	1.10	–0.72
	Western Alaska LCC	2.20	0.22	3.92	3.84	1.40	0.20	2.91
	Northwest Boreal LCC North	3.56	0.33	29.57	35.24	21.87	3.07	20.48
	Northwest Boreal LCC South	1.76	0.18	4.99	10.82	2.63	0.27	8.82
	North Pacific LCC	0.10	0.01	0.74	0.86	0.53	0.08	0.49
	Total	**11.22**	**1.11**	**46.73**	**54.09**	**29.15**	**4.71**	**31.99**
B1	Arctic LCC	1.22	0.13	6.30	4.19	3.96	0.99	0.21
	Western Alaska LCC	0.78	0.08	3.28	2.64	2.36	0.06	2.22
	Northwest Boreal LCC North	1.44	0.13	26.98	28.40	22.49	2.20	17.41
	Northwest Boreal LCC South	0.76	0.08	4.12	7.56	2.99	0.14	6.28
	North Pacific LCC	0.09	0.01	0.69	0.55	0.47	0.10	0.11
	Total	**4.29**	**0.42**	**41.36**	**43.34**	**32.26**	**3.49**	**26.23**

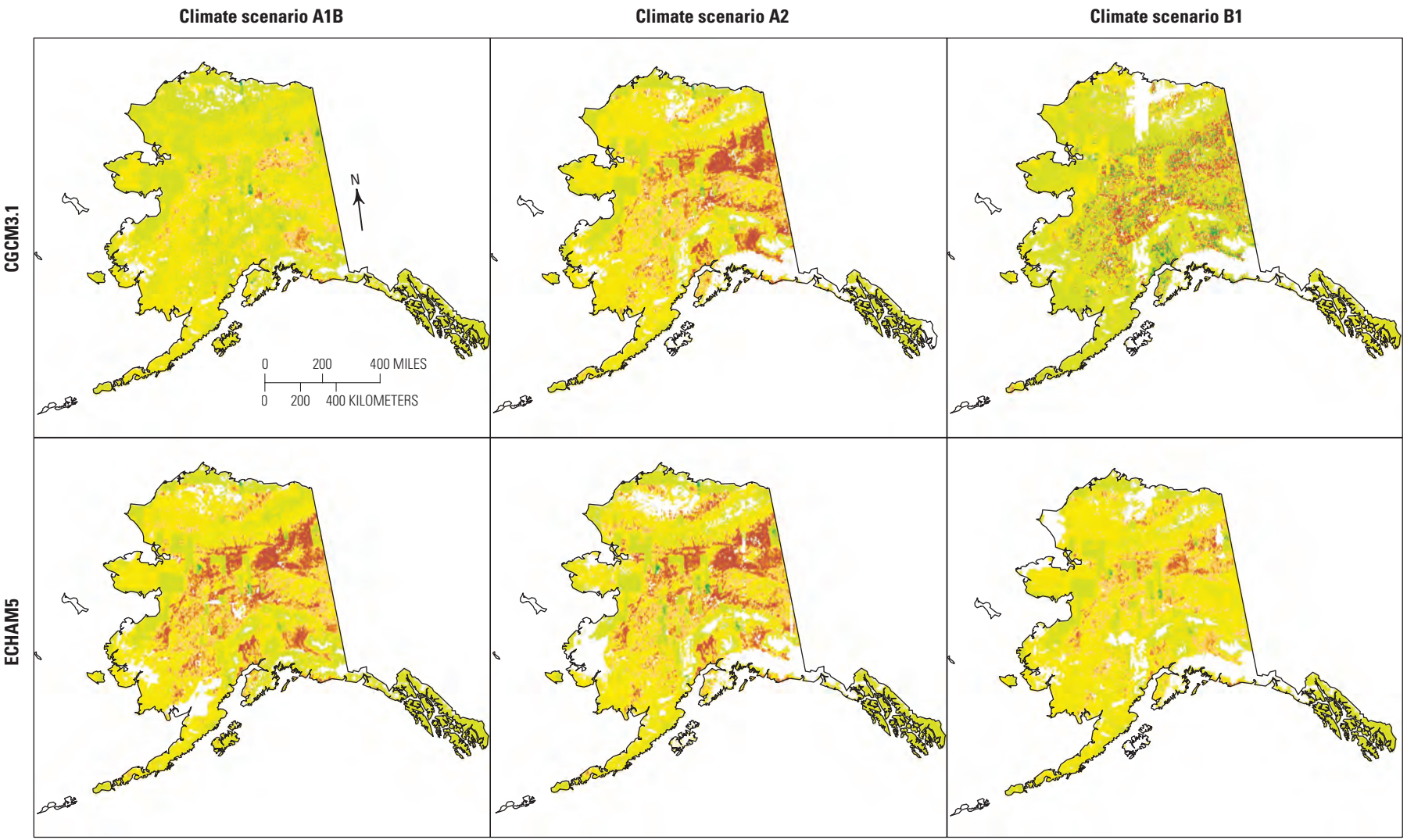

Figure 7.6. Spatial distribution of annual change in net methane emissions between the last decades of the historical period (2000–2009) and the projection period (2090–2099) for wetland ecosystems of Alaska for the two general circulation models, version 3.1-T47 of the Coupled Global Climate Model (CGCM3.1) developed by the Canadian Centre for Climate Modelling and Analysis and version 5 of the European Centre Hamburg Model (ECHAM5) developed by the Max Planck Institute, under three climate scenarios of the Intergovernmental Panel on Climate Change's Special Report on Emissions Scenarios (Nakićenović and Swart, 2000), B1, A1B, and A2, in order of low to high projected CO_2 emissions.

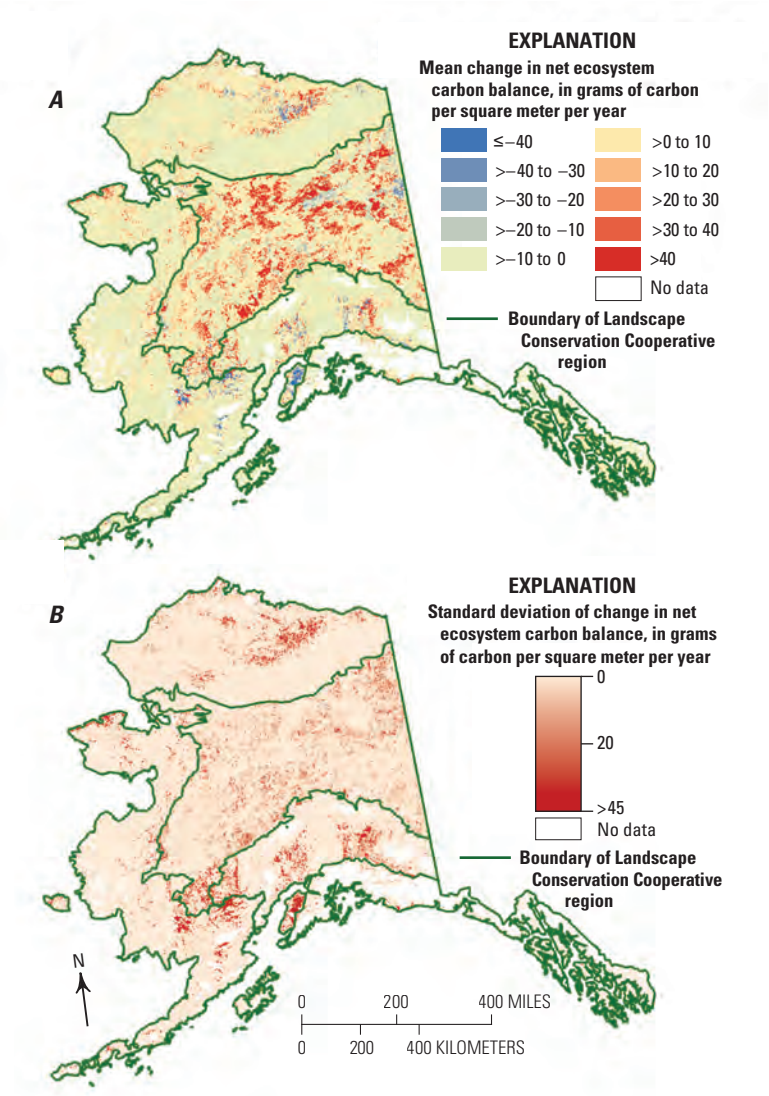

Figure 7.7. Spatial distribution of *A*, mean change in net ecosystem carbon balance between the last decades of the historical period (2000–2009) and the projection period (2090–2099) among the six climate simulations and *B*, corresponding standard deviation. The six climate simulations used in this report are combinations of two general circulation models, version 3.1-T47 of the Coupled Global Climate Model (CGCM3.1) developed by the Canadian Centre for Climate Modelling and Analysis and version 5 of the European Centre Hamburg Model (ECHAM5) developed by the Max Planck Institute, under three climate scenarios of the Intergovernmental Panel on Climate Change's Special Report on Emissions Scenarios (Nakićenović and Swart, 2000), B1, A1B, and A2, in order of low to high projected CO_2 emissions.

7.6. Conclusions

Alaska's wetland ecosystems were estimated to have produced net CH_4 emissions averaging 1 TgC/yr from 1950 through 2009. Biogenic CH_4 accounted for most (>90 percent) of the total emissions. Estimates of NECB during the historical period indicated that all LCC regions in Alaska were net carbon sinks except the Northwest Boreal LCC North. Carbon loss in the Northwest Boreal LCC North offset carbon gain from the other regions. As a result, 1.3 TgC/yr was lost during the historical period statewide—in addition to the 1 TgC/yr lost as CH_4, 0.3 TgC/yr was lost because of changes in NPP and wildfire emission—and the carbon loss was about equally distributed in the soil and the vegetation. The GWP of wetlands over the historical period indicated that wetlands were a significant source of greenhouse gas forcing at 33 $TgCO_2$-eq/yr.

The projected total CH_4 emissions across three anthropogenic CO_2 emissions scenarios and two GCMs were estimated to range from 36 to 90 $TgCO_2$-eq/yr by the 2090s, which represented an increase of 15 to 182 percent from the historical period. Comparatively, projected NPP ranged from 41.0 to 46.7 TgC/yr, which represented an increase of 10 to 25 percent from the historical period. Projected HR ranged from 26.4 to 34.0 TgC/yr, which represented a change of –3 to 25 percent from the historical period. Overall, by the end of the 21st century, carbon stocks in wetland ecosystems of all LCC regions of Alaska were projected to continue or start to grow. On average, wetland ecosystems would store 4.2 TgC/yr in 2090–2099, ranging from 3.0 to 5.3 TgC/yr statewide depending on climate simulation. Despite the uncertainty around the absolute value of projected NECB related to climate forcing, the trend of NECB is consistent among all six climate simulations, predicting that wetlands in Alaska will be a net carbon sink by 2099.

However, mainly because of the relatively large increase in CH_4 emissions during the projected period, GWP is projected to remain positive by the 2090s, ranging from 17.1 to 64.0 $TgCO_2$-eq/yr, which represented a change of –49 to 92 percent compared with the historical period. Atmospheric CO_2 concentration and mean annual temperature were identified to be the primary environmental controls of the projected increase in biogenic CH_4 emissions. The increase in vegetation productivity and subsequent increase in substrate for CH_4 production was the likely cause of the projected increased CH_4 production in response to climate change. This projected increase was enough to offset projected carbon storage in wetlands of Alaska during the 21st century. Furthermore, little is known about the environmental controls of thermokarst disturbance and its effect on local and regional carbon balance. For this reason, thermokarst disturbance was not included in the present assessment. However, field evidence suggests that changes in drainage conditions associated with thermokarst formation may increase CH_4 production and potentially increase the release of greenhouse gas in wetlands of Alaska.

7.7. References Cited

Chapin, F.S., III, Woodwell, G.M., Randerson, J.T., Rastetter, E.B., Lovett, G.M., Baldocchi, D.D., Clark, D.A., Harmon, M.E., Schimel, D.S., Valentini, R., Wirth, C., Aber, J.D., Cole, J.J., Goulden, M.L., Harden, J.W., Heimann, M., Howarth, R.W., Matson, P.A., McGuire, A.D., Melillo, J.M., Mooney, H.A., Neff, J.C., Houghton, R.A., Pace, M.L., Ryan, M.G., Running, S.W., Sala, O.E., Schlesinger, W.H., and Schulze, E.-D., 2006, Reconciling carbon-cycle concepts, terminology, and methods: Ecosystems, v. 9, no. 7, p. 1041–1050, http://dx.doi.org/10.1007/s10021-005-0105-7.

Clein, J.S., McGuire, A.D., Zhang, X., Kicklighter, D.W., Melillo, J.M., Wofsy, S.C., Jarvis, P.G., and Massheder, J.M., 2002, Historical and projected carbon balance of mature black spruce ecosystems across North America; The role of carbon-nitrogen interactions: Plant and Soil, v. 242, no. 1, p. 15–32, http://dx.doi.org/10.1023/a:1019673420225.

Euskirchen, E.S., Bret-Harte, M.S., Scott, G.J., Edgar, C., Shaver, G.R., 2012, Seasonal patterns of carbon dioxide and water fluxes in three representative tundra ecosystems in northern Alaska: Ecosphere, v. 3, no. 1, article 4, 19 p., http://dx.doi.org/10.1890/ES11-00202.1.

Fisher, J.B., Sikka, M., Oechel, W.C., Huntzinger, D.N., Melton, J.R., Koven, C.D., Ahlström, A., Arain, M.A., Baker, I., Chen, J.M., Ciais, P., Davidson, C., Dietze, M., El-Masri, B., Hayes, D., Huntingford, C., Jain, A.K., Levy, P.E., Lomas, M.R., Poulter, B., Price, D., Sahoo, A.K., Schaefer, K., Tian, H., Tomelleri, E., Verbeeck, H., Viovy, N., Wania, R., Zeng, N., and Miller, C.E., 2014, Carbon cycle uncertainty in the Alaskan Arctic: Biogeosciences, v. 11, p. 4271–4288, http://dx.doi.org/10.5194/bg-11-4271-2014.

Forster, Piers, Ramaswamy, Venkatachalam, Artaxo, Paulo, Berntsen, Terje, Betts, Richard, Fahey, D.W., Haywood, James, Lean, Judith, Lowe, D.C., Myhre, Gunnar, Nganga, John, Prinn, Ronald, Raga, Graciela, Schulz, Michael, and Van Dorland, Robert, 2007, Changes in atmospheric constituents and in radiative forcing, chap. 2 *of* Solomon, Susan, Qin, Dahe, Manning, Martin, Chen, Zhenlin, Marquis, Melinda, Averyt, Kristen, Tignor, M.M.B., and Miller, H.L., Jr., eds., Climate change 2007—The physical science basis; Contribution of Working Group I to the Fourth Assessment Report of the Intergovernmental Panel on Climate Change: Cambridge, United Kingdom, and New York, Cambridge University Press, p. 129–234. [Also available at http://www.ipcc.ch/publications_and_data/publications_ipcc_fourth_assessment_report_wg1_report_the_physical_science_basis.htm.]

French, N.H.F., Kasischke, E.S., and Williams, D.G., 2002, Variability in the emission of carbon-based trace gases from wildfire in the Alaskan boreal forest, Journal of Geophysical Research, v. 107, no. D1, p. FFR 7–1 to FFR 7–11, http://dx.doi.org/10.1029/2001JD000480.

Frolking, Steve, and Roulet, N.T., 2007, Holocene radiative forcing impact of northern peatland carbon accumulation and methane emissions: Global Change Biology, v. 13, no. 5, p. 1079–1088, http://dx.doi.org/10.1111/j.1365-2486.2007.01339.x.

Genet, H., McGuire, A.D., Barrett, K., Breen, A., Euskirchen, E.S., Johnstone, J.F., Kasischke, E.S., Melvin, A.M., Bennett, A., Mack, M.C., Rupp, T.S., Schuur, E.A.G., Turetsky, M.R., and Yuan, F., 2013, Modeling the effects of fire severity and climate warming on active layer thickness and soil carbon storage of black spruce forests across the landscape in interior Alaska: Environmental Research Letters, v. 8, no. 4, letter 045016, 13 p., http://dx.doi.org/10.1088/1748-9326/8/4/045016.

Gesch, D., Oimoen, M., Greenlee, S., Nelson, C., Steuck, M., and Tyler, D., 2002, The national elevation dataset: Photogrammetric Engineering and Remote Sensing, v. 68, no. 1, p. 5–11.

Gough, Laura, Moore, J.C., Shaver, G.R., Simpson, R.T., and Johnson, D.R., 2012, Above- and belowground responses of arctic tundra ecosystems to altered soil nutrients and mammalian herbivory: Ecology, v. 93, no. 7, p. 1683–1694, http://dx.doi.org/10.1890/11-1631.1.

Grand, J.B., Flint, P.L., and Heglund, P.J., 1997, Habitat use by nesting and brood rearing northern pintails on the Yukon-Kuskokwim Delta, Alaska: The Journal of Wildlife Management, v. 61, no. 4, p. 1199–1207, http://dx.doi.org/10.2307/3802117.

Harris, I., Jones, P.D., Osborn, T.J., and Lister, D.H., 2014, Updated high-resolution grids of monthly climatic observations—the CRU TS3.10 dataset: International Journal of Climatology, v. 34, no. 3, p. 623–642, http://dx.doi.org/10.1002/joc.3711.

He, Yujie, Jones, M.C., Zhuang, Qianlai, Bochicchio, Christopher, Felzer, B.S., Mason, Erik, and Yu, Zicheng, 2014, Evaluating CO_2 and CH_4 dynamics of Alaskan ecosystems during the Holocene Thermal Maximum: Quaternary Science Reviews, v. 86, p. 63–77, http://dx.doi.org/10.1016/j.quascirev.2013.12.019.

Homer, Collin, Huang, Chengquan, Yang, Limin, Wylie, Bruce, and Coan, Michael, 2004, Development of a 2001 National Land-Cover Database for the United States: Photogrammetric Engineering and Remote Sensing, v. 70, no. 7, p. 829–840, http://dx.doi.org/10.14358/PERS.70.7.829.

Ji, Lei, Zhang, Li, Rover, Jennifer, Wylie, B.K., and Chen, Xuexia, 2014, Geostatistical estimation of signal-to-noise ratios for spectral vegetation indices: ISPRS Journal of Photogrammetry and Remote Sensing, v. 96, p. 20–27, http://dx.doi.org/10.1016/j.isprsjprs.2014.06.013.

Ji, Lei, Zhang, Li, Wylie, B.K., and Rover, Jennifer, 2011, On the terminology of the spectral vegetation index (NIR–SWIR)/(NIR+SWIR): International Journal of Remote Sensing, v. 32, no.21, p. 6901–6909, http://dx.doi.org/10.1080/01431161.2010.510811.

Johnson, K.D., Harden, Jennifer, McGuire, A.D., Bliss, N.B., Bockheim, J.G., Clark, Mark, Nettleton-Hollingsworth, Teresa, Jorgenson, M.T, Kane, E.S., Mack, Michelle, O'Donnell, Jonathan, Ping, C.-L., Schuur, E.A.G., Turetsky, M.R., and Valentine, D.W., 2011, Soil carbon distribution in Alaska in relation to soil-forming factors: Geoderma, v. 167–168, p. 71–84, http://dx.doi.org/10.1016/j.geoderma.2011.10.006.

Jorgenson, M.T., and Osterkamp, T.E., 2005, Response of boreal ecosystems to varying modes of permafrost degradation: Canadian Journal of Forest Research, v. 35, no. 9, p. 2100–2111, http://dx.doi.org/10.1139/x05-153.

Jorgenson, M.T., Shur, Y.L., and Osterkamp, T.E., 2008, Thermokarst in Alaska, *in* Kane, D.L., and Hinkel, K.M., eds., Proceedings of the Ninth International Conference on Permafrost, Fairbanks, Alaska, June 29 to July 3, 2008: Institute of Northern Engineering, University of Alaska-Fairbanks, p. 869–876.

Jorgenson, Torre, Yoshikawa, Kenji, Kanevskiy, Mikhail, Shur, Yuri, Romanovsky, Vladimir, Marchenko, Sergei, Grosse, Guido, Brown, Jerry, and Jones, Ben, 2008a, Permafrost characteristics of Alaska, *in* Kane, D.L., and Hinkel, K.M., eds., Proceedings of the Ninth International Conference on Permafrost, Fairbanks, Alaska, June 29 to July 3, 2008: Institute of Northern Engineering, University of Alaska-Fairbanks, p. 121–122.

Jorgenson, Torre, Yoshikawa, Kenji, Kanevskiy, Mikhail, Shur, Yuri, Romanovsky, Vladimir, Marchenko, Sergei, Grosse, Guido, Brown, Jerry, and Jones, Ben, 2008b, Permafrost characteristics of Alaska (December 2008 update to July 2008 Ninth International Conference on Permafrost [NICOP] map): Fairbanks, Alaska, University of Alaska-Fairbanks, Institute of Northern Engineering, scale 1:7,200,000, http://permafrost.gi.alaska.edu/sites/default/files/AlaskaPermafrostMap_Front_Dec2008_Jorgenson_etal_2008.pdf.

Kasischke, E.S., and Turetsky, M.R., 2006, Recent changes in the fire regime across the North American boreal region—Spatial and temporal patterns of burning across Canada and Alaska: Geophysical Research Letters, v. 33, no. 9, letter L09703, 5 p., http://dx.doi.org/10.1029/2006GL025677.

Kivinen, J., Warmuth, M.K., and Auer, P., 1997, The Perceptron algorithm versus Winnow; Linear versus logarithmic mistake bounds when few input variables are relevant: Artificial Intelligence, v. 97, nos. 1–2, p. 325–343, http://dx.doi.org/10.1016/S0004-3702(97)00039-8.

Koven, C.D., Ringeval, Bruno, Friedlingstein, Pierre, Ciais, Philippe, Cadule, Patricia, Khvorostyanov, Dmitry, Krinner, Gerhard, and Tarnocai, Charles, 2011, Permafrost carbon-climate feedbacks accelerate global warming: National Academy of Sciences Proceedings, v. 108, no. 36, p. 14769–14774, http://dx.doi.org/10.1073/pnas.1103910108.

Lehner, Bernhard, and Döll, Petra, 2004, Development and validation of a global database of lakes, reservoirs and wetlands: Journal of Hydrology, v. 296, nos. 1–4, p. 1–22, http://dx.doi.org/10.1016/j.jhydrol.2004.03.028.

Liao, AnPing, Chen, LiJun, Chen, Jun, He, ChaoYing, Cao, Xin, Chen, Jin, Peng, Shu, Sun, FangDi, and Gong, Peng, 2014, High-resolution remote sensing mapping of global land water: Science China Earth Sciences, v. 57, no. 10, p. 2305–2316, http://dx.doi.org/10.1007/s11430-014-4918-0.

Lu, Huaxing, 2008, Modelling terrain complexity, *in* Zhou, Qiming, Lees, Brian, and Tang, Guo-an, eds., Advances in digital terrain analysis: Lecture Notes in Geoinformation and Cartography, p. 159–176, http://dx.doi.org/10.1007/978-3-540-77800-4_9.

Malone, Thomas, Liang, Jingjing, and Packee, E.C., 2009, Cooperative Alaska Forest Inventory: U.S. Department of Agriculture, Forest Service, Pacific Northwest Research Station, General Technical Report PNW–GTR–785, 42 p. [Also available at http://www.fs.fed.us/pnw/pubs/pnw_gtr785.pdf.]

Martin, P.D., Jenkins, J.L., Adams, F.J., Jorgenson, M.T., Matz, A.C., Payer, D.C., Reynolds, P.E., Tidwell, A.C., and Zelenak, J.R., 2009, Wildlife response to environmental Arctic change—Predicting future habitats of Arctic Alaska; Report of the Wildlife Response to Environmental Arctic Change (WildREACH) Predicting the Future Habitats of Arctic Alaska Workshop, Fairbanks, Alaska, November, 17–18, 2008: U.S. Fish and Wildlife Service, 138 p. [Also available at http://arcticlcc.org/assets/resources/WildREACH_Workshop_Report_Final.pdf.]

McFarlane, N.A., Boer, G.J., Blanchet, J.-P., and Lazare, M., 1992, The Canadian Climate Centre second-generation general circulation model and its equilibrium climate: Journal of Climate, v. 5, no. 10, p. 1013–1044, http://dx.doi.org/10.1175/1520-0442(1992)005<1013:TCCCSG>2.0.CO;2.

Myers-Smith, I.H., Harden, J.W., Wilmking, M., Fuller, C.C., McGuire, A.D., and Chapin, F.S., III, 2008, Wetland succession in a permafrost collapse; Interactions between fire and thermokarst: Biogeosciences, v. 5, no. 5, p. 1273–1286, http://dx.doi.org/10.5194/bg-5-1273-2008.

Nakićenović, Nebojša, and Swart, Robert, eds., 2000, Special report on emissions scenarios—A special report of Working Group III of the Intergovernmental Panel on Climate Change: Cambridge, United Kingdom, Cambridge University Press, 599 p. [Also available at http://www.ipcc.ch/ipccreports/sres/emission/index.php?idp=0.]

O'Donnell, J.A., Jorgenson, M.T., Harden, J.W., McGuire, A.D., Kanevskiy, M.Z., and Wickland, K.P., 2012, The effects of permafrost thaw on soil hydrologic, thermal, and carbon dynamics in an Alaskan peatland: Ecosystems, v. 15, no. 2, p. 213–229, http://dx.doi.org/10.1007/s10021-011-9504-0.

Rastetter, E.B., King, A.W., Cosby, B.J., Hornberger, G.M., O'Neill, R.V., and Hobbie, J.E., 1992, Aggregating fine-scale ecological knowledge to model coarser-scale attributes of ecosystems: Ecological Applications, v. 2, no. 1, p. 55–70, http://dx.doi.org/10.2307/1941889.

Roeckner, E., Bäuml, G., Bonaventura, L., Brokopf, R., Esch, M., Giorgetta, M., Hagemann, S., Kirchner, I., Kornblueh, L., Manzini, E., Rhodin, A., Schlese, U., Schulzweida, U., and Tompkins, A., 2003, The atmospheric general circulation model ECHAM5, part I—Model description: Max-Planck-Institut für Meteorologie Report, no. 349, 127 p. [Also available at https://www.mpimet.mpg.de/fileadmin/publikationen/Reports/max_scirep_349.pdf.]

Roeckner, E., Brokopf, R., Esch, M., Giorgetta, M., Hagemann, S., Kornblueh, L., Manzini, E., Schlese, U., and Schulzweida, U., 2004, The atmospheric general circulation model ECHAM5, part II—Sensitivity of simulated climate to horizontal and vertical resolution: Max-Planck-Institut für Meteorologie Report No. 354, 56 p. [Also available at http://pubman.mpdl.mpg.de/pubman/item/escidoc:995221:8/component/escidoc:995220/MPI_Report354.pdf.]

Roy, D.P., Ju, Junchang, Kline, Kristi, Scaramuzza, P.L., Kovalskyy, Valeriy, Hansen, Matthew, Loveland, T.R., Vermote, Eric, and Zhang, Chunsun, 2010, Web-enabled Landsat Data (WELD); Landsat ETM+ composited mosaics of the conterminous United States: Remote Sensing of Environment, v. 114, no. 1, p. 35–49, http://dx.doi.org/10.1016/j.rse.2009.08.011.

Rupp, T.S., Chen, Xi, Olson, Mark, and McGuire, A.D., 2007, Sensitivity of simulated boreal fire dynamics to uncertainties in climate drivers: Earth Interactions, v. 11, no. 3, p. 1–21, http://dx.doi.org/10.1175/EI189.1.

Rupp, T.S., Starfield, A.M., and Chapin, F.S., III, 2000, A frame-based spatially explicit model of subarctic vegetation response to climatic change; Comparison with a point model: Landscape Ecology, v. 15, no. 4, p. 383–400, http://dx.doi.org/10.1023/A:1008168418778.

Rupp, T.S., Starfield, A.M., Chapin, F.S., III, and Duffy, P., 2002, Modeling the impact of black spruce on the fire regime of Alaskan boreal forest: Climatic Change, v. 55, no. 1–2, p. 213–233, http://dx.doi.org/10.1023/A:1020247405652.

Schaefer, Kevin, Zhang, Tingjun, Bruhwiler, Lori, and Barrett, A.P., 2011, Amount and timing of permafrost carbon release in response to climate warming: Tellus; Series B, Chemical and Physical Meteorology, v. 63B, no. 2, p. 165–180, http://dx.doi.org/10.1111/j.1600-0889.2011.00527.x.

Schuur, E.A.G., Bockheim, James, Canadell, J.G., Euskirchen, Eugenie, Field, C.B., Goryachkin, S.V., Hagemann, Stefan, Kuhry, Peter, Lafleur, P.M., Lee, Hanna, Mazhitova, Galina, Nelson, F.E., Rinke, Annette, Romanovsky, V.E., Shiklomanov, Nikolay, Tarnocai, Charles, Venevsky, Sergey, Vogel, J.G., and Zimov, S.A., 2008, Vulnerability of permafrost carbon to climate change; Implications for the global carbon cycle: BioScience, v. 58, no. 8, p. 701–714, http://dx.doi.org/10.1641/b580807.

Shaver, G.R., and Chapin, F.S., III, 1986, Effect of fertilizer on production and biomass of tussock tundra, Alaska, U.S.A.: Arctic and Alpine Research, v. 18, no. 3, p. 261–268. [Also available at http://dx.doi.org/10.2307/1550883.]

Shaver, G.R., and Chapin, F.S., III, 1991, Production; Biomass relationships and element cycling in contrasting arctic vegetation types: Ecological Monographs, v. 61, no. 1, p. 1–31, http://dx.doi.org/10.2307/1942997.

Sistla, S.A., Moore, J.C., Simpson, R.T., Gough, Laura, Shaver, G.R., and Schimel, J.P., 2013, Long-term warming restructures Arctic tundra without changing net soil carbon storage: Nature, v. 497, no. 7451, p. 615–618, http://dx.doi.org/10.1038/nature12129.

Stocker, T.F., Qin, Dahe, Plattner, G.-K., Tignor, M.M.B., Allen, S.K., Boschung, Judith, Nauels, Alexander, Xia, Yu, Bex, Vincent, and Midgley, P.M., eds., 2013, Summary for policymakers, *in* Climate change 2013—The physical science basis, Contribution of Working Group I to the Fifth Assessment Report of the Intergovernmental Panel on Climate Change: Cambridge, United Kingdom, Cambridge University Press, p. 3–29. [Also available at http://www.ipcc.ch/report/ar5/wg1/.]

Sullivan, P.F., Sommerkorn, Martin, Rueth, H.M., Nadelhoffer, K.J., Shaver, G.R., and Welker, J.M., 2007, Climate and species affect fine root production with long-term fertilization in acidic tussock tundra near Toolik Lake, Alaska: Oecologia, v. 153, no. 3, p. 643–652, http://dx.doi.org/10.1007/s00442-007-0753-8.

Sutton, C.D., 2005, Classification and regression trees, bagging, and boosting: Handbook of Statistics, v. 24, p. 303–329, http://dx.doi.org/10.1016/S0169-7161(04)24011-1.

Turetsky, M.R., Kane, E.S., Harden, J.W., Ottmar, R.D., Manies, K.L., Hoy, Elizabeth, and Kasischke, E.S., 2011, Recent acceleration of biomass burning and carbon losses in Alaskan forests and peatlands: Nature Geoscience, v. 4, no. 1, p. 27–31, http://dx.doi.org/10.1038/ngeo1027.

Turetsky, M.R., Treat, C.C., Waldrop, M.P., Waddington, J.M., Harden, J.W., and McGuire, A.D., 2008, Short-term response of methane fluxes and methanogen activity to water table and soil warming manipulations in an Alaskan peatland: Journal of Geophysical Research; Biogeosciences, v. 113, no. G3, article G00A10, 15 p., http://dx.doi.org/10.1029/2007JG000496.

Van Wijk, M.T., Williams, M., Gough, L., Hobbie, S.E., and Shaver, G.R., 2003, Luxury consumption of soil nutrients; A possible competitive strategy in above-ground and below-ground biomass allocation and root morphology for slow-growing arctic vegetation?: Journal of Ecology, v. 91, no. 4, p. 664–676, http://dx.doi.org/10.1046/j.1365-2745.2003.00788.x.

Whitcomb, Jane, Moghaddam, Mahta, McDonald, Kyle, Kellndorfer, Josef, and Podest, Erika, 2009, Mapping vegetated wetlands of Alaska using L-band radar satellite imagery: Canadian Journal of Remote Sensing, v. 35, no. 1, p. 54–72, http://dx.doi.org/10.5589/m08-080.

Yi, Shuhua, Manies, Kristen, Harden, Jennifer, and McGuire, A.D., 2009, Characteristics of organic soil in black spruce forests; Implications for the application of land surface and ecosystem models in cold regions: Geophysical Research Letters, v. 36, no. 5, letter L05501, 5 p., http://dx.doi.org/10.1029/2008GL037014.

Yi, Shuhua, McGuire, A.D., Harden, Jennifer, Kasischke, Eric, Manies, Kristen, Hinzman, Larry, Liljedahl, Anna, Randerson, Jim, Liu, Heping, Romanovsky, Vladimir, Marchenko, Sergei, and Kim, Yongwon, 2009, Interactions between soil thermal and hydrological dynamics in the response of Alaska ecosystems to fire disturbance: Journal of Geophysical Research; Biogeosciences, v. 114, no. G2, article G02015, 20 p., http://dx.doi.org/10.1029/2008JG000841.

Yi, Shuhua, McGuire, A.D., Kasischke, Eric, Harden, Jennifer, Manies, Kristen, Mack, Michelle, and Turetsky, Merritt, 2010, A dynamic organic soil biogeochemical model for simulating the effects of wildfire on soil environmental conditions and carbon dynamics of black spruce forests: Journal of Geophysical Research; Biogeosciences, v. 115, no. G4, article G04015, 15 p., http://dx.doi.org/10.1029/2010JG001302.

Yuan, F.-M., Yi, S.-H., McGuire, A.D., Johnson, K.D., Liang, J., Harden, J.W., Kasischke, E.S., and Kurz, W.A., 2012, Assessment of boreal forest historical C dynamics in the Yukon River Basin; Relative roles of warming and fire regime change: Ecological Applications, v. 22, no. 8, p. 2091–2109, http://dx.doi.org/10.1890/11-1957.1.

Zhuang, Q., McGuire, A.D., Melillo, J.M., Clein, J.S., Dargaville, R.J., Kicklighter, D.W., Myneni, R.B., Dong, J., Romanovsky, V.E., Harden, J., and Hobbie, J.E., 2003, Carbon cycling in extratropical terrestrial ecosystems of the Northern Hemisphere during the 20th century; A modeling analysis of the influences of soil thermal dynamics: Tellus; Series B, Chemical and Physical Meteorology, v. 55B, no. 3, p. 751–776, http://dx.doi.org/10.1034/j.1600-0889.2003.00060.x.

Zhuang, Q., McGuire, A.D., O'Neill, K.P., Harden, J.W., Romanovsky, V.E., and Yarie, J., 2002, Modeling soil thermal and carbon dynamics of a fire chronosequence in interior Alaska: Journal of Geophysical Research; Atmospheres, v. 107, no. D1, p. FFR 3–1 to FFR 3–26, http://dx.doi.org/10.1029/2001jd001244.

Zhuang, Q., Melillo, J.M., Kicklighter, D.W., Prinn, R.G., McGuire, A.D., Steudler, P.A., Felzer, B.S., and Hu, S., 2004, Methane fluxes between terrestrial ecosystems and the atmosphere at northern high latitudes during the past century; A retrospective analysis with a process-based biogeochemistry model: Global Biogeochemical Cycles, v. 18, no. 3, article GB3010, 23 p., http://dx.doi.org/10.1029/2004GB002239.

Zhuang, Q., Romanovsky, V.E., and McGuire, A.D., 2001, Incorporation of a permafrost model into a large-scale ecosystem model; Evaluation of temporal and spatial scaling issues in simulating soil thermal dynamics: Journal of Geophysical Research; Atmospheres, v. 106, no. D24, p. 33649–33670, http://dx.doi.org/10.1029/2001jd900151.